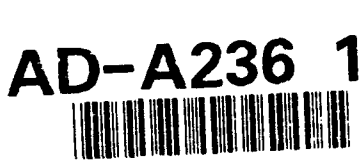

The Pennsylvania State University
APPLIED RESEARCH LABORATORY
P.O. Box 30
State College, PA 16804

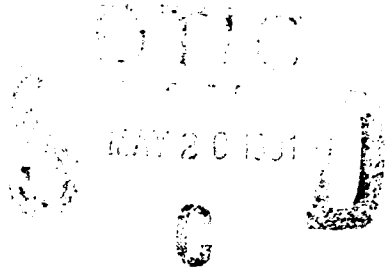

MULTICHANNEL ADAPTIVE VIBRATION CONTROL OF A MOUNTED PLATE

by

Lance B. Bischoff
Scott D. Sommerfeldt

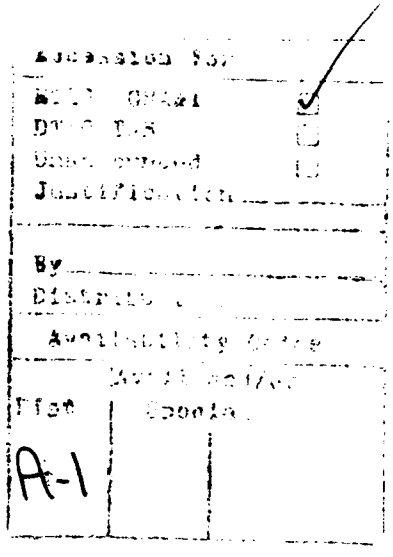

Technical Report No. TR 91-005
May 1991

Supported by:
Space and Naval Warfare Systems Command

L.R. Hettche, Director
Applied Research Laboratory

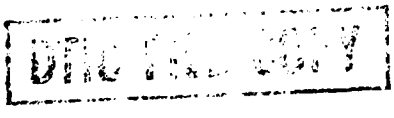

REPORT DOCUMENTATION PAGE

Form Approved
OMB No. 0704-0188

1. AGENCY USE ONLY (Leave blank)	2. REPORT DATE	3. REPORT TYPE AND DATES COVERED
	May 1991	

4. TITLE AND SUBTITLE
Multichannel Adaptive Vibration Control of a Mounted Plate

5. FUNDING NUMBERS
N00039-88-C0051

6. AUTHOR(S)
L. B. Bishoff, S. D. Sommerfeldt

7. PERFORMING ORGANIZATION NAME(S) AND ADDRESS(ES)
Applied Research Laboratory
Penn State University
P. O. Box 30
State College, PA 16804

8. PERFORMING ORGANIZATION REPORT NUMBER
TR-91-005

9. SPONSORING / MONITORING AGENCY NAME(S) AND ADDRESS(ES)
Space and Naval Warfare Systems Command
Department of the Navy
Washington, DC 20363-5100

10. SPONSORING / MONITORING AGENCY REPORT NUMBER

11. SUPPLEMENTARY NOTES

12a. DISTRIBUTION / AVAILABILITY STATEMENT
Approved for public release; distribution unlimited

12b. DISTRIBUTION CODE

13. ABSTRACT *(Maximum 200 words)*

This thesis investigates the possibility of actively controlling a plate, mounted to a rigid foundation with springs. A multichannel adaptive control system, based on the least-mean-squares (LMS) algorithm, has been developed and applied to the transmission paths of this mechanical plate system. Experimental results are presented for the case of single and multiple-frequency excitation. Feedback compensation is developed to remove any feedback in the control system, and thus avoid any instabilities caused by such feedback. The effect of this control on vibrating modal patterns is presented and thus gives insight to global as well as to localized effects of active control. It is shown that this multichannel adaptive control system presents an excellent means of controlling low frequency vibration transmission where passive techniques fail.

The issue of stability of a coupled system, such as a plate, is addressed and a solution is presented. In addition, stability and convergence properties of multiadaptive processes are presented. The result is that convergence parameters of each separate adaptive process have to be carefully selected, with respect to other convergence parameters, in order to avoid system instabilities.

14. SUBJECT TERMS
active control, plate, multichannel, LMS algorithm, stability, feedback compensation

15. NUMBER OF PAGES
90

16. PRICE CODE

17. SECURITY CLASSIFICATION OF REPORT	18. SECURITY CLASSIFICATION OF THIS PAGE	19. SECURITY CLASSIFICATION OF ABSTRACT	20. LIMITATION OF ABSTRACT
Unclassified	Unclassified	Unclassified	SAR

Abstract

This thesis investigates the possibility of actively controlling a plate, mounted to a rigid foundation with springs. A multichannel adaptive control system, based on the least-mean-squares (LMS) algorithm, has been developed and applied to the transmission paths of this mechanical plate system. Experimental results are presented for the case of single and multiple frequency excitation. Feedback compensation is developed to remove any feedback in the control system, and thus avoid any instabilities caused by such feedback. The effect of this control on vibrating modal patterns is presented and thus gives insight to global as well as to localized effects of active control. It is shown that this multichannel adaptive control system presents an excellent means of controlling low frequency vibration transmission where passive techniques fail.

The issue of stability of a coupled system, such as a plate, is addressed and a solution is presented. In addition, stability and convergence properties of multiadaptive processes are presented. The result is that convergence parameters of each separate adaptive process have to be carefully selected, with respect to other convergence parameters, in order to avoid system instabilities.

Table of Contents

List of Figures

List of Tables

Chapter 1

INTRODUCTION

Active vibration control is an excellent example of modern research and development applied to a problem that is common to many structures. Vibrations can be undesirable in many situations, and are sometimes not easy to control. Vibration sources usually contact a structure in more than one location, and can cause complex vibration patterns. Through an interdisciplinary approach, which ties together many areas of research in science and engineering, this thesis presents a solution to a class of realistic vibration problems.

1.1 Early History

The concepts used for this adaptive control project are based on ideas and advancements made as far back as 1933. At that time, Lueg filed a patent for his "Process of Silencing Sound Oscillations" [1,2]. His invention was to lay the groundwork for this, as well as other active control projects.

Lueg's invention was intended to cancel propagating sound waves in a duct by destructive interference. The sound waves were sensed by a microphone, passed through an amplifier with an adjustable gain, and added back into the duct through a loudspeaker which could be moved in order to adjust phase relationships. The amplifier and speaker were then adjusted until the loudspeaker output was 180 degrees out of phase with the sound wave in the duct. This was a considerable advancement for the technology available at that time, but was limited in many ways. The phase had to be readjusted for different frequencies of interest, and the output of his system was limited due to feedback oscillations. This made the system very difficult to control, as well as impractical to implement. Twenty years later, while working at RCA electronics, Olson expanded on Lueg's work [3,4] by placing the controlling loudspeaker in a box filled with acoustic absorbing material, creating a monopole source. By placing his sensing microphone in the nearfield of the controlling loudspeaker, and using a feedback control system, he was able to produce a "zone of silence." This system also suffered practical limitations, however, due to its localized effective range and instabilities associated with feedback control.

Both Lueg's and Olson's efforts were valuable as they showed the feasibility of reducing energy in the field by means of a secondary source. The major limitations that they experienced were simply technology and controllability. Some sort of system needed to be developed in which system stability was constantly maintained, and system performance was constantly maximized.

1.2 Modern Advancements

The early 1970s showed improvements on Lueg's work by the use of multiple speaker arrangements to produce sound propagation in the forward direction to cancel the unwanted noise, while producing no backward propagating sound waves [5,6,7,8]. In the late 1970s active control was interfaced with signal processing to improve system stability. Chaplin and Smith [9] used the impulse response of their control system and convolved it with the controller's input signal, obtaining a better control signal for driving the loudspeaker. This system was used to reduce exhaust noise produced by diesel engines and produced more desirable results than were previously obtainable.

With advancements being made in digital computers, a new door was being opened to the field of active control. Adaptive filtering, prediction and control techniques were being developed and successfully applied [10]. With the use of faster computers, the performance of these algorithms was extensively studied for discrete-time systems. The application of this adaptive theory to active control provided solutions for problems such as system identification, and optimal performance of the controller. Due to time varying system parameters, however, careful attention to system stability had to be maintained. The mathematics that these adaptive algorithms were based on was computationally complex, requiring large amounts of computer time. In order for real-time adaptive algorithms to be applied to acoustic problems, it was desirable to shorten the required computational time.

The earliest suitable application of adaptive noise cancellation was achieved by

Widrow, *et al.* [11,12]. His system was computationally simple and produced excellent results in attenuating unwanted noise in electrical signals. Widrow used a steepest descent type method of adaptation called the Least-Mean-Squares (LMS) algorithm to identify the optimal control filter for separating interfering signals from wideband information signals. This technique was applied to many different applications including beam-forming of antenna arrays, electrical interference cancellation of electrocardiograms, echo cancellation of telephone lines, and other applications where unwanted signals needed to be separated from desired information, thus producing better signal to noise ratios. This gradient-based LMS algorithm has been used extensively in real-time adaptive control of acoustic fields, due to its simplicity. This algorithm constantly adapts its control filter transfer function until the corresponding error signal is minimized. Its application to a number of active control problems is fairly straightforward since this error signal can be measured at a point were maximum attenuation is desired. The rate at which this error signal is minimized depends on a number of parameters, including the nature of the algorithm itself.

As development of electronic controlling methods grew in the early 1980s, so did research in the area of geometric configurations for active control, and the interface between the controller and the physical system. Warnaka *et al.* [13,14,15,16] investigated the acoustic mixing of active attenuators with propagating waves in ducts. Their methods used an acoustic waveguide to connect the controlling loudspeaker to the noise field, for frequencies below the cross-modes of the ducts. They showed that limitations of the controlling loudspeaker, i.e. temperature, its physical size, etc., could be isolated from the

noise field. Further research by Warnaka *et al.* investigated the limitations of electronic controllers and how to minimize them by the use of what they referred to as "time-sharing" of cascaded stages of the controller. Their system provided excellent results for the cases of broadband signals, transient responses, and reduction in interior spaces.

Nelson *et al.* [17,18] investigated the use of multiple controlling sources in achieving total reduction by the means of active control. Their research looked into optimal location of such loudspeaker arrangements for different geometrical configurations. The results of this research proved that global reduction could be achieved if the controlling sources where located within a half wavelength of the noise source, for the corresponding frequencies of interest. Although it is desirable to cancel noise at the source, it is sometimes impractical to implement. Their efforts also looked into theoretically establishing what the *absolute capability* would be for reducing sound levels by active means.

Application of active control has proven successful in canceling sound waves in ducts and enclosures. It has also been proven effective in the field of active vibration control [19-31]. Both of these areas deal with high speed signal processing, particularly in the case of vibrations. Propagation times through solids are generally very short, requiring rapid determination of control signals. In fact, due to the dispersive medium, there is usually a cut-off frequency at which the time required to calculate and actuate the control signal surpasses the time for the excitation signal to propagate through the structure. For such applications, technology is once again a limiting factor.

Recently [32], Sommerfeldt investigated the ability to actively control a two-stage

vibration isolation mount so as to reduce transmitted vibrations to the foundation at the single mounting point. This research led to the development of an actual mechanical system and an adaptive algorithm to achieve such control. This algorithm was generalized to be applicable for the case of multichannel control and led directly to the development of this thesis.

1.3 Description of the Problem

This thesis describes a real-time adaptive control scheme which has been developed for active vibration control of a plate. The problem was directed at investigating a realistic mounting situation in which multichannel adaptive control is desired to attenuate vibrations of a distributed system, i.e. a plate. Most mounting systems include multiple points of contact between the source and foundation. If vibration control is applied to these mounting points, force transmission to the foundation is minimized, assuming a rigid foundation and assuming the mounts behave as lumped elements.

The mechanical system for this study is a rectangular metal plate mounted on a rigid foundation, with springs located near each of its four corners. Mechanical input to the system is provided by inertial forces, meaning the shaking mechanisms do not contact the foundation in any way, so as not to transmit any further vibrations to the foundation. The controlling actuators are located as near to the corners as practical. By locating the actuators at the corners, control limitations which occur if the actuators are located at

nodal points of the corresponding modes, are minimized. The plate is then excited to several of its bending modes, and attenuation at the mounting points is attempted through adaptive control. This plate is intended to be representative of a structure such as an electric motor, internal-combustion engine, or any other vibration source that is attached in some way to a foundation. This thesis demonstrates improvements in the performance of already existing mounting techniques for such systems, and offers solutions to low frequency problems associated with them.

1.4 Overview of the Thesis

Chapter 2 presents an analysis of the control system. The plate alone with its boundary conditions represents a complex vibration problem, and is not solved by classical means. Instead the vibration patterns and their corresponding frequencies are predicted by methods compiled by Leissa [33]. Mass loading effects due to the control shakers are analyzed in this section, and predicted effectiveness of the controller is investigated. Chapter 3 examines the development of the algorithm used by the controller to achieve adaptive control. System stability requirements are discussed in this chapter and effects of system parameters on the convergence rates are predicted. Chapter 4 briefly discusses the actual experimental apparatus used to achieve measurable results. Chapter 5 is the concentration of this thesis, as it contains actual results of the experiments. This chapter shows the differences between 1, 2, and 4 channel control effectiveness and their corresponding convergence properties. It shows how feedback

compensation affects the performance of the controller. Finally, this chapter shows measured plots of the modal patterns associated with the vibrating plate, both with control on and off. Chapter 6 contains concluding remarks on the limitations and applications of the active vibration control system. This last chapter also includes recommendations for future research towards the advancement of active vibration control.

Chapter 2

VIBRATION ANALYSIS OF THE PLATE SYSTEM

Before any control is introduced to this problem, attention should be given to the vibrations that the system, consisting of the plate, mounts, and control actuators, will be experiencing. This experimental model of a plate mounted to a foundation with multiple springs, and controlled at the corners by inertial forces, represents a resilient mounting system. Such a system will resonate at the frequencies corresponding to the lumped-mass-spring system resonance, the bending resonance frequencies of the plate, and the resonance of the controlling shakers. The lumped-mass-spring and shaker resonances are straightforward to predict; however, the resonance frequencies of the plate, and the modal patterns associated with them, are complicated to analyze, and beyond the intent of this thesis. It is, however, important to estimate these vibration patterns in order to predict the effectiveness of the controller when applied to the plate. Variables such as nodal line location, modal density, and modal overlap all play important roles in determining the response of the mechanical system to control.

2.1 Difficulties of a Free Plate

The springs used in this mounting apparatus are rather compliant, and the first plate used is rather massive; therefore, this plate can be approximated as having completely free boundary conditions. Effects of the controlling shakers will be temporarily neglected for ease of analysis. The general solution of a rectangular plate [34], with dimensions a and b and thickness h, can be written as

$$\begin{aligned} W(x,y) = {} & A_1 \sin\alpha x \sin\gamma y + A_2 \sin\alpha x \cos\gamma y \\ & + A_3 \cos\alpha x \sin\gamma y + A_4 \cos\alpha x \cos\gamma y \\ & + A_5 \sinh\alpha_i x \sinh\gamma_i y + A_6 \sinh\alpha_i x \cosh\gamma_i y \\ & + A_7 \cosh\alpha_i x \sinh\gamma_i y + A_8 \cosh\alpha_i x \cosh\gamma_i y, \end{aligned} \tag{2.1}$$

where

$$\alpha^2 + \gamma^2 = \alpha_i^2 + \gamma_i^2 = \beta^2$$

$$\beta^4 = \frac{\omega^2 \rho}{D_E}$$

$$D_E = \frac{Eh^3}{12(1-\nu^2)}$$

$$0 < x < a$$

$$0 < y < b.$$

In the above equation, ω represents the frequency in radians, ρ is the density per unit area, ν is Poisson's ratio, and E is the Young's modulus of the material. Due to the fact that the above equation is complex, α and α_i correspond to the complex wave number in the x-direction, and γ and γ_i correspond to the complex wave number in the y-direction.

To determine the constants A_i, α_m and γ_n, one must substitute in the boundary conditions associated with the appropriate system. If two opposite edges of a rectangular plate are simply supported, the solution $W(x,y)$ can be separated into two functions $X(x)$ and $Y(y)$. If two opposite edges are not simply supported, the solution can not be separated, and it is not possible to calculate modal patterns of the plate using analytical methods. In the case of a completely free plate, the solution is not separable, and thus classical analytical methods are not feasible.

This problem, as well as other inseparable solution problems have been studied by various people. Leissa [33] compiled a number of these studies into one paper and changed their notations accordingly, so as to have one paper with identical notation and explanations for many different boundary conditions and geometrical configurations. From Leissa's work, it is possible to predict modal patterns and their corresponding frequencies, by knowing the material of the plate, its dimensions, and the appropriate boundary conditions. Although there is some small amount of error associated with Leissa's tables, they are accurate enough to approximate the resonance frequencies of the plate and the corresponding modes of the plate.

Leissa's results were used to estimate the resonance frequencies of two different plates used in this thesis. The first plate consisted of a one-half inch thick aluminum plate, while the second plate was a steel plate with a thickness of one sixteenth of an inch. The aluminum plate was used to represent a relatively rigid structure, with only a few bending modes in the frequency range of interest. The steel plate was designed to have a higher modal density and could thus be used to examine the ability of the

controller to attenuate several modes at the same time. The predicted resonance frequencies and measured resonance frequencies of both the aluminum and steel plates are given in Table 2.1 and Table 2.2, respectively. The parameters used [35] to calculate these values, assuming completely free boundary conditions for a rectangular plate, are also given. It should be noted that the measured values in Table 2.1 were measured with the shakers attached to the thick aluminum plate. This is not the case for Table 2.2, where the shakers were removed for the measured values. Also noted is the fact that the 2,3 mode of the aluminum plate was above the frequency range of the controller and therefore not measured within the bandwidth of the spectrum analyzer.

2.2 Modal Analysis

In investigating the modes of the system, it should be noted that only odd (or even, depending on notation) modes are strongly excited in the apparatus used. Due to the size of the excitation shaker (representing the vibration source) and space limitations imposed by the foundation, the only reasonable attachment location in the y direction (the shorter dimension) was at the center of this dimension. For purposes of symmetry, the shaker was also located in the center of the x dimension (the longer dimension), and thus located at the center of the plate. Modes with nodal lines through the center of the plate are therefore difficult to excite. Taking this into consideration, one would expect excitation of the uncontrolled plate to produce vibration patterns associated with a completely free plate, that is, antinodes near the edges where the mounting springs are

Table 2.1: Resonances of Aluminum Plate

Mode	Predicted Frequency	Measured Frequency	Predicted Error	Measured Error
2,2	169.9 Hz	120.0 Hz	5.81%	29.3%
3,1	182.3 Hz	170.0 Hz	3.56%	6.75%
3,2	393.8 Hz	310.0 Hz	4.37%	21.3%
1,3	424.5 Hz	380.0 Hz	0.09%	10.5%
4,1	491.2 Hz	475.0 Hz	5.96%	3.3%
2,3	569.7 Hz	--------	-1.67%	--------

$E=7.1\times10^{10}$ Pa $\rho_s=2700$ Kg/m^3 $\nu=0.3$

$h=0.0127$ m $a=0.6096$ m $b=0.4064$ m

Table 2.2: Resonances of Steel Plate

Mode	Predicted Frequency	Measured Frequency	Predicted Error	Measured Error
2,2	20.8 Hz	20.0 Hz	5.81%	4.00%
3,1	22.4 Hz	24.0 Hz	3.56%	7.14%
3,2	48.3 Hz	47.5 Hz	4.37%	1.66%
1,3	52.1 Hz	57.0 Hz	0.09%	9.40%
4,1	60.3 Hz	60.5 Hz	5.96%	0.33%
2,3	69.9 Hz	72.5 Hz	-1.67%	3.72%

$E=19.5\times10^{10}$ Pa $\quad \rho_s=7700$ Kg/m^3 $\quad \nu=0.3$

$h=1.59\times10^{-3}$ m $\quad a=0.6096$ m $\quad b=0.4064$ m

located. This provides large amplitude vibrations that would be transmitted to the foundation if uncontrolled. As the excitation frequencies get higher, and the mode shapes more complex, phase differences between each of the corners exist. This can also cause complex coupling problems from corner to corner, that must also be accounted for when control is applied. Thus it is felt that this apparatus provides an excellent experimental model to study the effects and performance of active control.

The effect of the controlling actuators on the mechanical system can be viewed as a change in the boundary conditions. If vibrations are minimized at the error sensors of the controlling system, the boundary conditions approach that of a plate with zero displacement at the points where the error sensors are located. Thus distinct changes in modal patterns might be expected with control on versus control off.

2.3 Predicted Effects of Control

Due to the imposing of point constraints at the locations of the error sensors, control should basically result in nodal lines passing through the error sensors. This could result either by shifting the nodal lines of the original mode, or by driving the plate into a different mode. This makes for rather complicated changes of modal patterns to analyze by classic analytical methods of vibration study.

Although an analytical study of the system is formidable, certain effects can be predicted for the experimental investigation. The location of the controlling actuators and error sensors, with respect to nodal locations of the uncontrolled plate, will play an

important role in the effectiveness of the control system. If the actuators are located near nodal lines, for instance, their ability to absorb energy (i.e. match the vibrations 180 degrees out of phase) is greatly reduced, since the vibration amplitude experienced at those points is minimal to begin with. Therefore, modes with nodal lines at the control points, can not be easily controlled. The result in such a case may be an unchanged modal pattern, with slight localized reduction at the controlling points.

The predicted effectiveness is improved when the control actuators are located closer to displacement antinodes. In this case, it is predicted that the modal pattern will be altered so as to provide nodal lines at the error sensor locations. The ability to provide a reduction in vibrations at such frequencies is therefore predicted to be promising. For these conditions, the controlling mechanisms are more efficient and can provide more dynamic range before their linear operating range is exceeded. This is an important consideration, as the controlling shakers must operate linearly in order to ensure that the system remains stable.

For the case of multichannel control, coupling between the control sources can be expected. This means that control applied at one location on the plate will also have an effect at other locations on the plate. In the case of control, localized reduction at one corner may cause an increase in vibrations at another corner. If multichannel control is to take place, these coupling effects must be accounted for. However, if properly compensated for, the multichannel control system should produce better results than single-channel control, as it allows the controller to couple into more modes of the plate. The most obvious benefit of such a control scheme is that the combined masses of the

controlling shakers provide better low frequency response for the control system. However, at higher frequencies, where less mass is required for the control actuators, their independent phase relationships allow them to absorb more energy at their corresponding contact points. The possibilities of multichannel control also include a less localized reduction, and possibly, a more global reduction of the plate's vibrations.

Chapter 3

THE CONTROL ALGORITHM

Due to the fact that this thesis investigates the use of an adaptive system to control vibration fields, stability of the adaptive system must be established. The active sources provide disturbances which are fed back through the physical system to the controller input sensor. To guarantee stability, this feedback must be compensated for, while attempting to maximize the performance of the controller. An adaptive controller is an appealing solution, as it can compensate for changing system parameters, input signal changes, feedback, system resonances, and other problems associated with active control.

In recent years, much research in the field of adaptive control has taken place, as outlined in chapter 1. As computer technology has grown, so has the processing speed of computers. This has made it possible to study different adaptive schemes and note their good and bad qualities through system simulations. Although many different algorithms have been presented, the first real application towards electronic noise control was carried out by Widrow *et al.* [11]. Widrow developed the LMS (Least Mean Squares) algorithm, with his main emphasis being computational simplicity. Since noise and vibration control requires real-time control, it is desirable to keep the mathematics of the controlling scheme simple. In real-time control, a signal is sampled and an output

or driving signal to the controlling mechanism must be calculated during that sample period. This sampling happens at high speed during which the calculations of the algorithm must also take place. In the case of this thesis, a minimum sampling rate of 1 kHz is chosen. It is for this reason that the LMS algorithm has been chosen for this active control topic.

3.1 The Finite Impulse Response Filter

Before description of the adaptive algorithm is given, an explanation of the filtering process is described. The Finite Impulse Response (FIR) filter is straightforward to implement with the aid of a computer. An FIR filter can be implemented as a delay line with numerical constants, known as filter coefficients, multiplying the appropriately delayed data. By summing the outputs of these multiplications, certain filter characteristics can be achieved. FIR filters are desirable in this experiment, as they have no feedback associated with them, and are therefore always stable, if the input is stable. Linear phase characteristics are achievable, and the frequency response of the filter can be determined through the use of the Z-transform. If the coefficients of such a filter are changed, the frequency response of that filter changes accordingly. Thus by properly adjusting the filter coefficients, while the filter is operating, it can be thought of as adapting to the situation. Proper adaptation of the coefficients for this thesis is controlled by the LMS algorithm.

3.2 The LMS Algorithm

The LMS algorithm is a steepest descent type algorithm which arrives at an optimal solution by iteration, providing certain conditions are met. In this thesis, the LMS algorithm's weighting coefficients are implemented as tap delay coefficients in a FIR digital filter. When the output of this FIR filter, denoted as $\hat{d}(n)$, is added to the desired (or undesired in the case of active cancellation) signal of the system, denoted as $d(n)$, there will be a prediction error, which depends upon how well the filter approximates the system, given by

$$e(n) = d(n) + \hat{d}(n). \tag{3.1}$$

In this notation, n represents an incremental discrete time index, corresponding to the sample period number. Since the output of the LMS filter is obtained from an FIR filter, it can be written as

$$\hat{d}(n) = X_N^T(n) W_N(n), \tag{3.2}$$

where $\mathbf{X_N}$, represented in vector notation by

$$X_N^T(n) \equiv [x(n)\ \ x(n-1) \cdots x(n-N+1)], \tag{3.3}$$

corresponds to values of the delayed input signal, and $\mathbf{W_N}$, represented in vector notation by

$$W_N^T(n) \equiv [w_0(n)\ \ w_1(n) \cdots w_{N-1}(n)], \tag{3.4}$$

corresponds to the N weighting coefficients of the LMS filter. Thus, the LMS prediction error can be expressed as

$$e(n) = d(n) + X_N^T(n) W_N(n). \tag{3.5}$$

This prediction error is used to adjust the weighting coefficients so as to minimize the squared error signal.

The minimization process can be more easily understood if the Mean Squared Error (MSE) is thought of as a N+1 -dimensional surface, where N is the number of weighting coefficients. In the case of an LMS algorithm with two weighting coefficients, this mean squared error surface, can be thought of as a "bowl" (see Figure 3.1), where the X- and Y-axes correspond to the two weighting coefficients, and the Z-axis corresponds to the value of the mean squared error. The iterative procedure adjusts these N weighting coefficients according to the negative gradient or "slope" of this error surface to reach an optimal value W_N^* located at "the bottom of the bowl." These weighting coefficients are multiplied by corresponding values of the delayed input signal, as shown in equation (3.2), arriving at a filter output signal described in section 3.1. The output signal of the filter is then mixed into the error summation point where it is superimposed upon the desired (or undesired) signal, resulting in destructive interference, and thus cancellation of the desired signal.

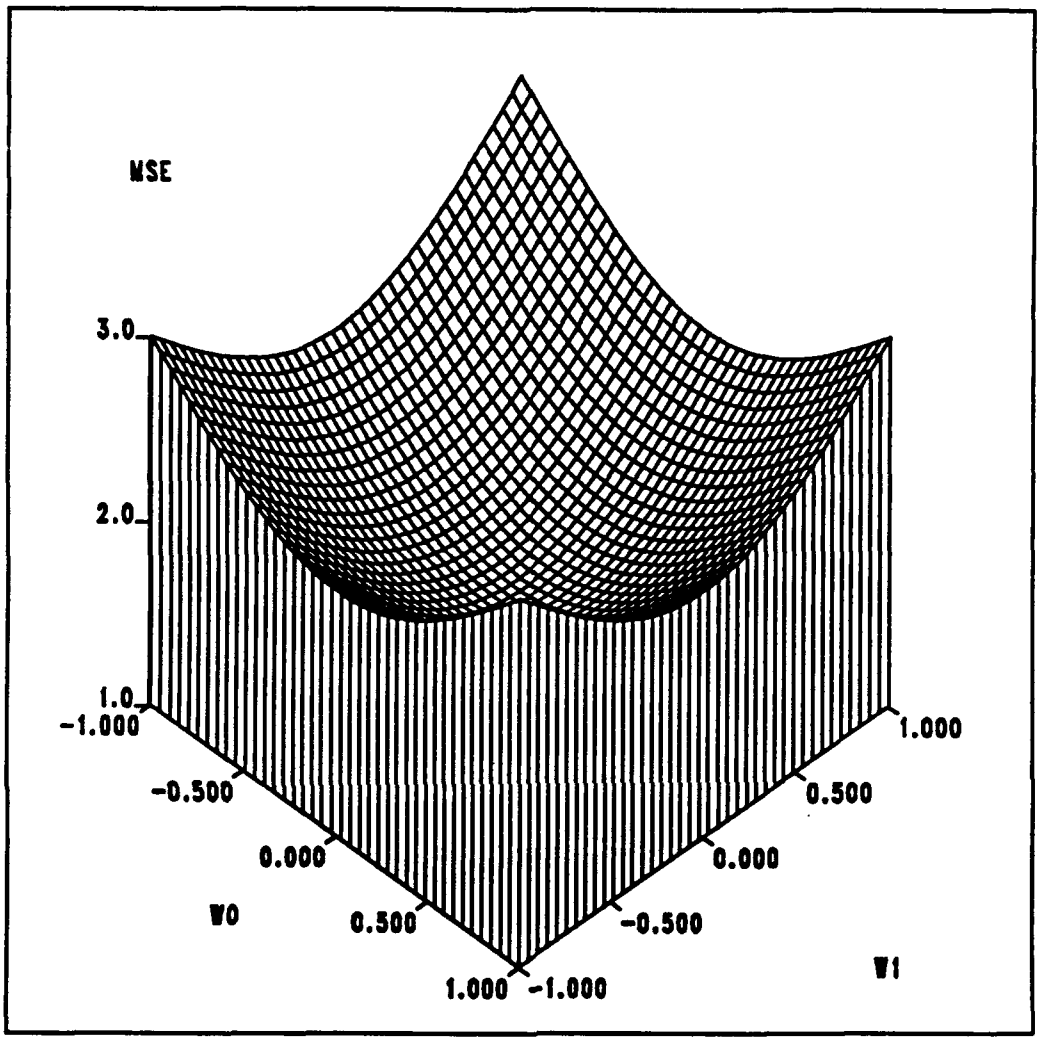

Figure 3.1: Mean Squared Error surface

The MSE is defined as the expectation, or ensemble average, of the squared error and is represented by

$$\varepsilon(n) = E\{e^2(n)\}, \tag{3.6}$$

where $E\{\}$ denotes the expectation operator. In order to determine the form of a steepest descent algorithm, the gradient of the MSE must be calculated.

Because *a priori* knowledge of the signal is rarely known, it is impractical to calculate the expectation of the MSE during real-time operation. One solution to this problem is to use the instantaneous value of the squared error as an estimate for the expected value. This is the estimate that the LMS algorithm is based upon. If the negative gradient of the instantaneous squared error is calculated, and the filter coefficients are updated according to this negative gradient, the LMS algorithm update equation for the weighting vector is obtained,

$$W_N(n+1)=W_N(n)-2\mu e(n)X_N(n), \tag{3.7}$$

where $X_N(n)$ represents the input signal to the filter.

The variable μ in equation (3.7) is a convergence parameter, selected to maintain system stability. Within this stability region it is desirable to select μ so that the algorithm converges at a reasonable rate, with minimal *misadjustment error* [36] (defined later). In order to determine the stability region for μ, the input autocorrelation matrix is defined as

$$R=E\{X_N(n)\ X_N^T(n)\}. \tag{3.8}$$

Earlier work by Widrow *et al.* [11] has shown that the weighting coefficient vector will converge to its optimal value W^*, generally called the Wiener solution [37], and remain stable as long as the convergence parameter is greater than zero, but less than the reciprocal value of the largest eignvalue of the autocorrelation matrix R:

$$0 < \mu < \frac{1}{\lambda_{max}}. \tag{3.9}$$

If the MSE versus the number of iterations is plotted, an exponentially decaying learning curve which levels off at a minimum MSE value results, provided a stable value for μ is chosen. Figure 3.2 shows the learning curve and was obtained using actual values of the squared error signal for the case of a 1-channel control system. This control system was actually the filtered-*x* algorithm (to be discussed later) and figure 3.2 is plotted on a 3-to-1 average, for data reduction purposes. The time constant for this convergence curve is inversely related to the value of μ.

Since the LMS algorithm only approximates the true gradient of the MSE surface, there is some noise associated with estimating the optimal weight vector, $W_N^*(n)$. This excess MSE is referred to as *misadjustment noise*, and is caused by the instantaneous LMS weight "jitter" about their mean value. The actual value of this excess MSE has been shown [36] to equal

$$\sigma_x^2 \mu \varepsilon_{min} \sum_{i=1}^{N} (1 - \mu\lambda_i)^{-1}, \tag{3.10}$$

where σ_x^2 is equal to the mean square power of the input signal. As seen, the power of this misadjustment noise is related to both the value chosen for μ and the input signal data.

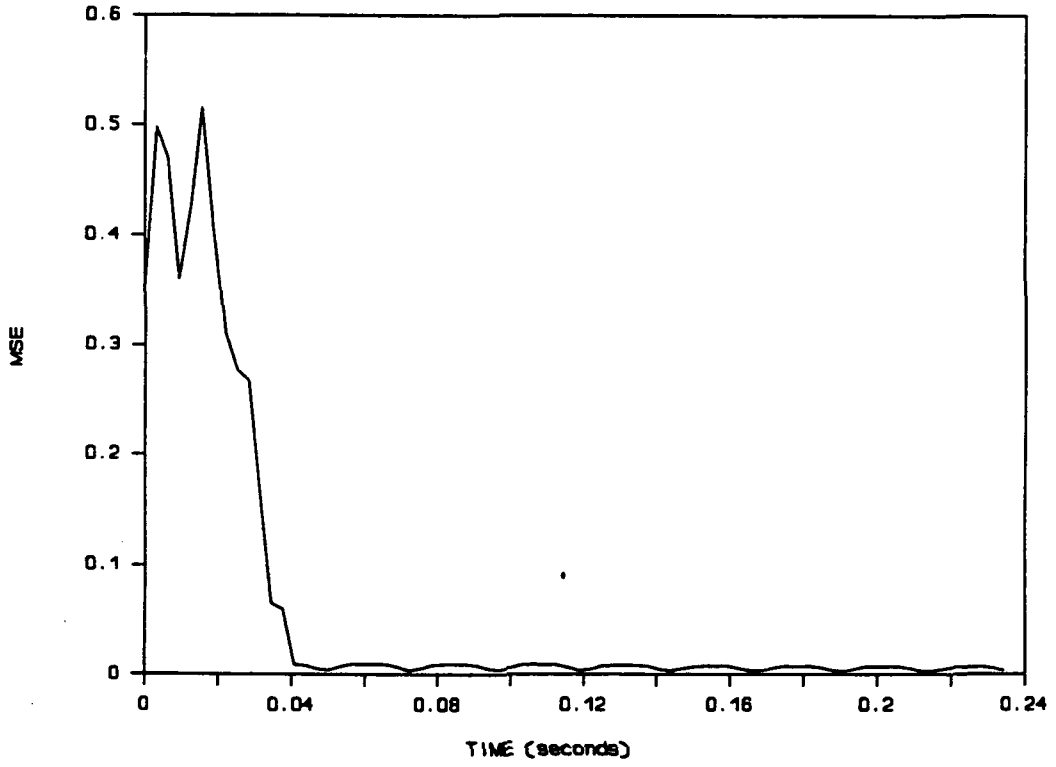

Figure 3.2: MSE learning curve

It is for these reasons that μ must be selected carefully. The first consideration is that a stable value must be chosen in order to guarantee convergence of the algorithm. The next consideration is convergence speed versus misadjustment noise. This represents two conflicting ideas, so that a trade-off between the two is involved in the selection of the convergence parameter.

Another noise problem to address is additive noise, regardless of the excitation source, and is referred to as plant noise. The plant noise is viewed as additive noise to the input of the adaptive filter, uncorrelated with the desired signal. In a control application, the error signal to the LMS algorithm is available after control has been

applied to the system, and the response measured. Thus the plant, for an active vibration control problem, can represent the transfer functions through signal conditioning hardware and the mechanical system. The adaptive process will have no effect on this plant noise, while converging to the Wiener solution. Thus, significant plant noise may result in inadequate control.

Widrow and Stearns developed the "filtered-x" algorithm [38] to compensate for this additive noise. In the development of this algorithm they represented the plant as a transfer function. In active control, this plant corresponds to the physical situation. This method allows the adaptive filter to be placed forward of the plant in a cascade sequence, as seen in Figure 3.3. In an active control problem, the adaptive filter is naturally forward of the plant. In this way the input to the LMS update equation is no longer the measured desired signal $x(n)$, but a filtered version of it

$$r(n-i) \equiv \sum_{k=0}^{K-1} h_k(n) x(n-k-i), \tag{3.11}$$

where $h_k(n)$ represents tap coefficients of a system identification filter with transfer function characteristics of the signal conditioning hardware and the mechanical system. In this way the plant noise is no longer an input to the adaptive filter. This can be thought of as system identification and must be properly modeled to ensure optimal performance, as well as stability, of the controller. An appealing solution to proper modelling of the system is another adaptive process which can be updated iteratively. In this way, time varying system parameters, such as phase speed through the mechanical

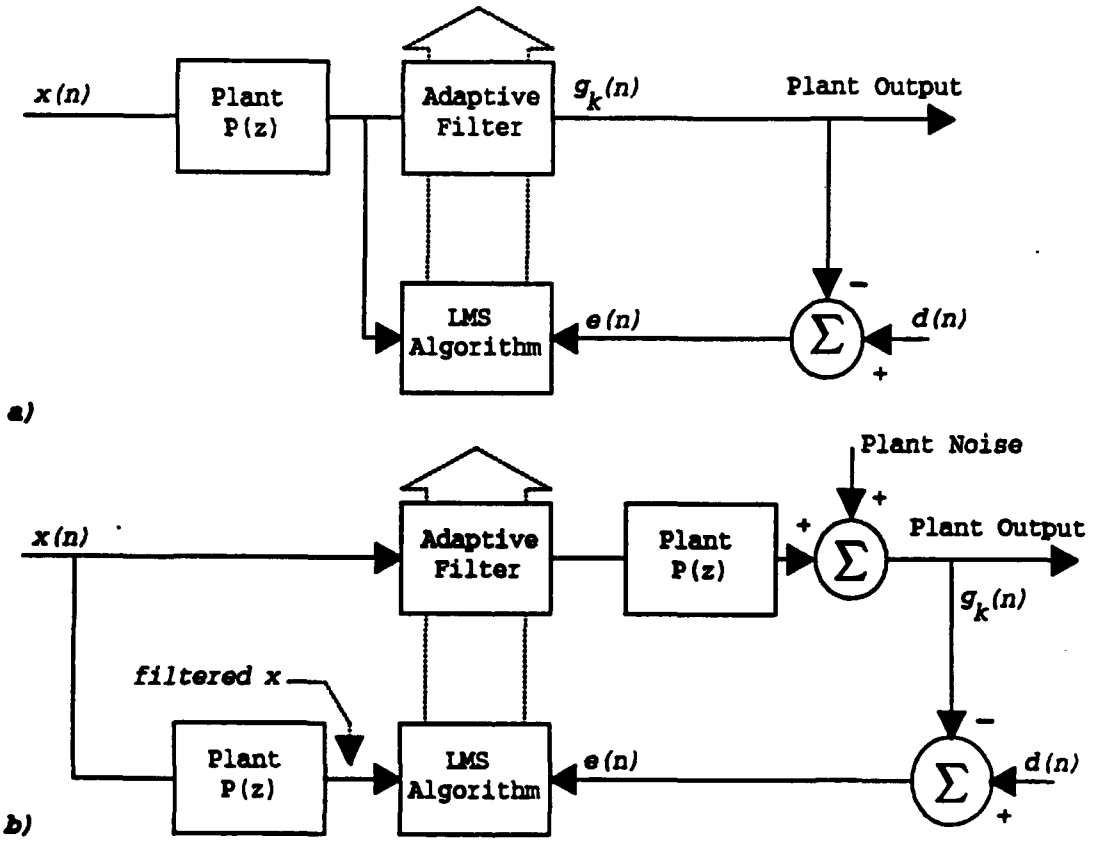

Figure 3.3: Filtered-*X* algorithm. a)uncompensated plant b)plant placed forward of LMS algorithm.

system due to temperature fluctuations, may be accurately modelled and thus compensated for.

3.3 The Projection Algorithm

One problem associated with actual implementation of adaptive processing in acoustical control problems involves system identification. In developing the LMS algorithm, it was assumed that the output of the controller was the same as the input to the error summation point. This is not true in active control situations and must be compensated for to ensure system stability. In the case of multichannel control, each individual control channel is coupled to all of the error sensors, and must be considered to successfully maintain stability. The filtered-x algorithm can properly compensate for problems with inherent transfer functions from the control filter to the error sensor, providing proper modelling of the system transfer function occurs. It is for this reason that an adaptive scheme known as the projection algorithm, or Normalized Least-Mean-Squares (NLMS) algorithm [39], was used.

The transfer function from the controller's output to the error summation point input can represent delay times and filtering characteristics associated with D/A converters, filters, amplifiers, and propagation through the physical system. The actual transfer function is represented in block diagram form as **H** (see Figure 3.4).

In the case of L error sensors, or channels, the output of the LMS filter, previously denoted as $\hat{a}(n)$ can now be written in vector form **Y** in order to represent past values of

each channel's output,

$$\begin{aligned} \mathbf{Y}^T(n) \equiv [\, & y_1(n)\ y_1(n-1)\cdots y_1(n-K+1) : \\ & y_2(n)\ y_2(n-1)\cdots y_2(n-K+1) : \\ & \cdots y_M(n)\ y_M(n-1)\cdots y_M(n-K+1)], \end{aligned} \tag{3.12}$$

where M represents the number of control actuators or outputs of the system. Since **H** represents a transfer function it will be modelled as another FIR filter of tap length M *times* K. It will filter the output of the controlling LMS filter as was seen in Figure 3.4.

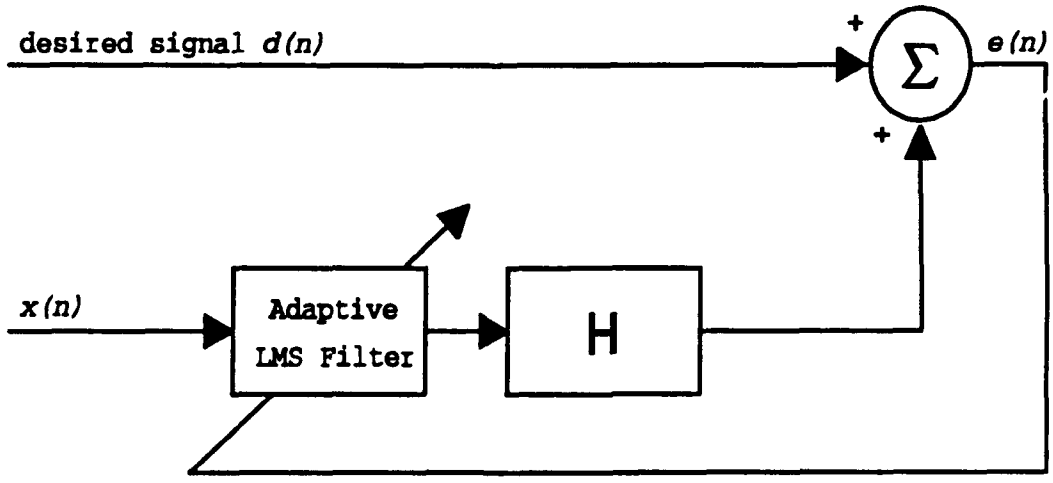

Figure 3.4: Block diagram of system

Thus the new approximation to the desired signal $d(n)$, will have its corresponding

error signal represented in multichannel notation, with subscript l notating the channel number as follows:

$$e_l(n) = d_l(n) + \sum_{m=1}^{M}\sum_{k=0}^{K-1} h_{lmk}(n)\sum_{i=0}^{N-1} w_{mi}(n-k)x(n-i-k), \tag{3.13}$$

where,

$$l=1,2,...L.$$

In this case h_{lmk} represents the system identification coefficients and can also be represented in vector form as

$$\begin{aligned} \mathbf{H}_l^T(n) \equiv [&h_{l10}(n)\ h_{l11}(n)\cdots h_{l1(K-1)}(n) \vdots \\ &h_{l20}(n)\ h_{l21}(n)\cdots h_{l2(K-1)}(n) \vdots \\ &\cdots h_{lM0}(n)\ h_{lM1}(n)\cdots h_{lM(K-1)}(n)]. \end{aligned} \tag{3.14}$$

The desired signal, $d_l(n)$, can be assumed to be correlated with delayed values of the input signal. Therefore, the relationship between the input and desired signal can be modelled with another FIR filter. $\mathbf{H}_l^T(n)$ models the transfer function from the LMS filter output signal to the corresponding lth error sensor. The input desired signal model is used to cancel the effects of the system, as described in the filtered-x algorithm, at the input to the lth LMS update equation. Appending $\mathbf{H}_l^T(n)$ with the input desired signal model, allows redefinition of the vectors in equations (3.12) and (3.14) in the following notation:

$$\Theta_l^T(n) \equiv [h_{l10}(n)\cdots h_{lM(K-1)} : h_{l(M+1)0}(n)\cdots h_{l(M+1)(K-1)}(n)] \tag{3.15}$$

$$\Phi^T(n) \equiv [y_1(n)\cdots y_N(n-K+1) : x(n)\ x(n-1)\cdots x(n-K+1)]. \tag{3.16}$$

This makes for an easy representation, previously defined for the single channel case in equation (3.5), of the lth error signal as follows:

$$e_l(n) = \Theta_l^T(n)\Phi(n). \tag{3.17}$$

Thus it can be shown [39] that the coefficients of the projection algorithm can be updated iteratively, in a simple calculation according to

$$\hat{\Theta}_l(n+1) = \hat{\Theta}_l(n) + \frac{a\Phi(n)}{b + \Phi^T(n)\Phi(n)}\left[\Theta_l^T(n)\Phi(n) - \hat{\Theta}_l^T(n)\Phi(n)\right], \tag{3.18}$$

where

b > 0 prevents division by 0

a = projection mu, 0 < a < 2 to ensure convergence

$\Theta_l^T(n)\Phi(n)$ = measured *l*th error signal

$\hat{\Theta}_l^T(n)\Phi(n)$ = estimated *i*th error signal.

Since actual values, corresponding to delayed sequences of control and input signals, are readily available, as are the values corresponding to actual error signals, the projection algorithm is suitable for implementation in real time control.

3.4 A Priori Feedback Compensation

Feedback must be compensated for in any active control system in order to counteract any system resonances associated with the path from the controlling mechanisms to the input sensor. In the case of multichannel active control, observability of feedback through the system becomes increasingly difficult as the number of channels grows, due to coupling effects of the system. When these multiple controlling mechanisms are working in unison, it is difficult to determine which, if any, are working in an unstable region. It is for this reason that feedback paths are calculated *a priori* in this experiment.

The method is performed by running a signal, preferably white noise, into each of the controlling mechanisms separately. At the same time, the sensor to be used as input to the adaptive algorithm, is first used as the error sensor for a separate adaptive filter. These separate filters, one for each feedback path, are allowed to adapt for a reasonable length of time, with the only input to the mechanical system originating from the corresponding control actuator. After adaptation, the adaptive filters are set as simple FIR filters, with their transfer function characteristics matching those of their corresponding feedback path. During real-time control, the output of these fixed FIR filters will closely match the signal which is fed back through the system to the input sensor. By subtracting the output of the FIR filters from the input sensor signal, the feedback can be largely removed. A block diagram showing the setup procedure is

shown in Figure 3.5 and a block diagram showing how each feedback compensator is used, is shown in Figure 3.6.

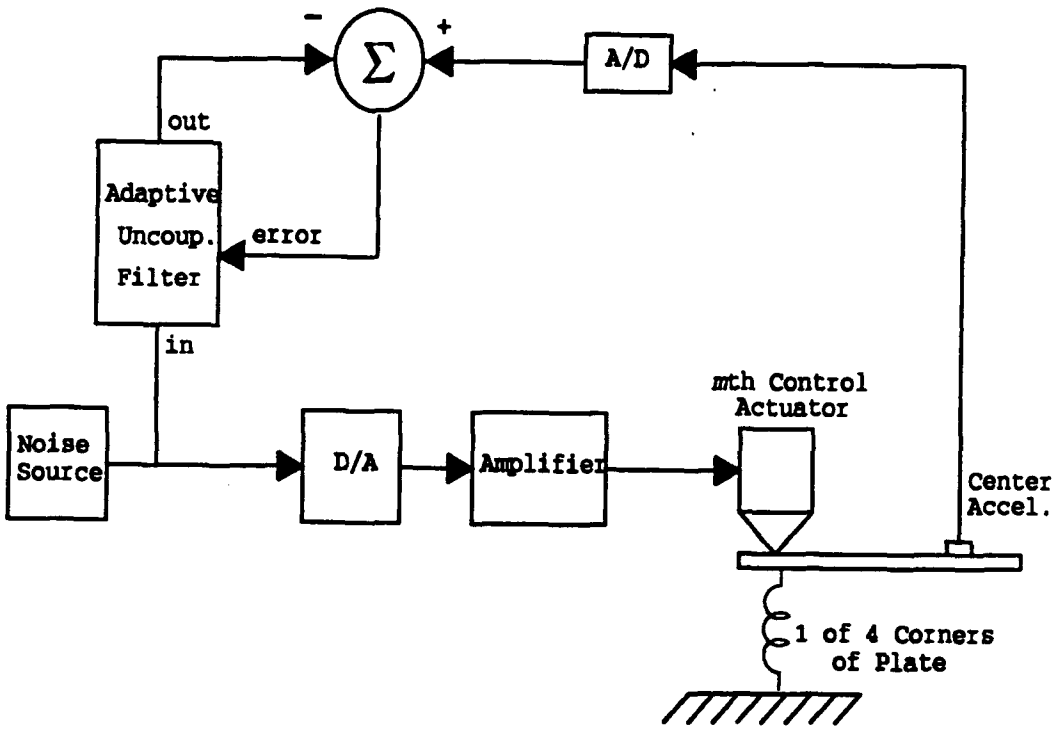

Figure 3.5: Block diagram for adapting uncoupling filter.

These feedback compensation filters are implemented in hardware. The outputs of each of these filters are summed, and the sum subtracted from the input signal to the control algorithm, thus removing feedback from the input signal. In this way, feedback compensation is carried out without excessive computer time being used. Such hardware is currently available, and will be discussed in detail in section 4.2 of this thesis.

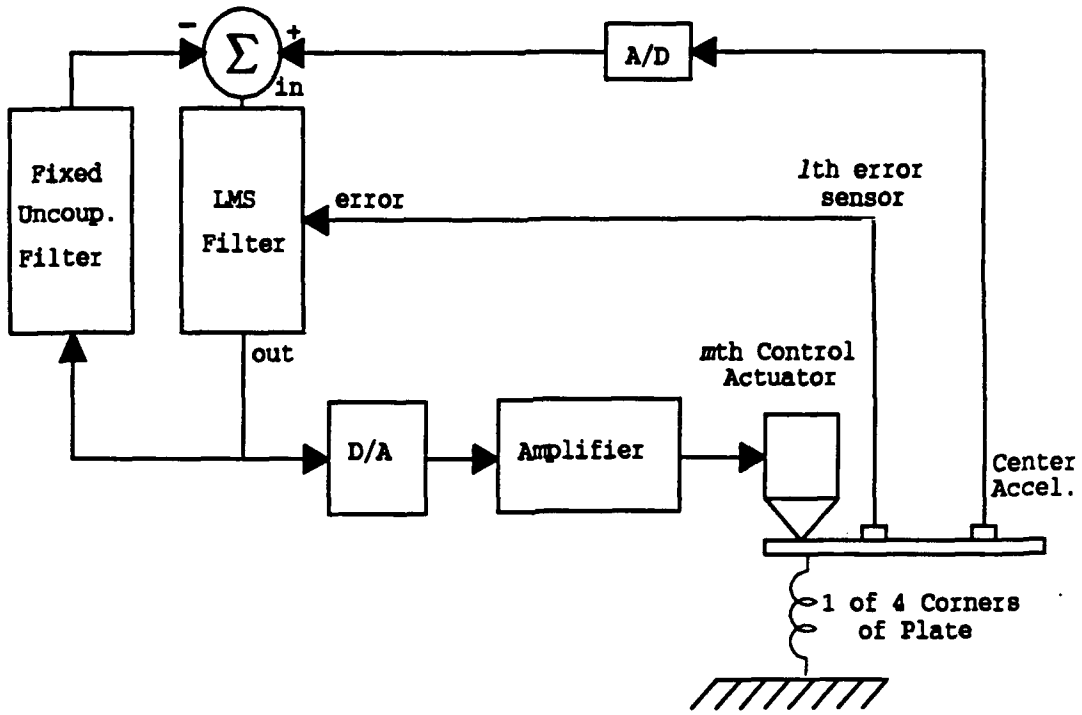

Figure 3.6: Block diagram for using uncoupling filter.

3.5 Adaptive Mu Algorithm

Due to the multiple feedback paths of this system, instability may be approached at a rapid rate. If a value of μ nearing the stability point of the system is chosen, the adaptive algorithm may not have a chance to recover. This is the case when trying to maximize the convergence rate and must be accounted for when trying to achieve such results. The value of μ corresponds to the rate of change at which the LMS filter's taps are updated. If the system is approaching an unstable region, and the convergence parameter is too high, the algorithm may overshoot this unstable region and will thus not

recover from such an error. If however the value of μ is decreased when approaching an instability, the taps of the LMS filter will be changed less rapidly, allowing the controlling algorithm to recover and return to a more stable region of control. This is what is referred to as the adaptive μ, or Joint Complex Gradient Transversal Filter algorithm [40].

It will later be seen that a reasonable value of μ may be calculated based upon the input signal power at the time the algorithm is executed. This is a value corresponding to the maximum stable μ available. As long as the average input power does not change and the value of μ does not exceed this μ_{max}, stability should be the result. However, as mentioned before, the fine stability point may be exceeded when trying to maximize convergence times. The value of μ may therefore be updated iteratively, based upon a moving average value of the input power. Since delayed values of input power are readily available, implementation is possible in this algorithm without a great amount of computational complexity. If $\mathbf{R}_{xx}(0)$ is to represent the input signal strength, an increase in its value will cause a decrease in the value calculated for μ (see equation (3.27)). If this were not an adaptive process, the value chosen for $\mathbf{R}_{xx}(0)$ would be based upon the input signal strength at the execution time of the algorithm and would therefore produce a constant value somewhat less than μ_{max}. This thesis, however, uses an adaptive process and the value for μ is calculated in real time based on the input signal strength according to

$$R_{xx}(0) \approx \frac{255}{256}\sum_{i=1}^{255} x^2(n-i) + \frac{1}{256}\, x^2(n), \qquad (3.19)$$

where the past 256 values of the input signal are known. In this way, if the input signal at sample period n starts to increase in strength, indicating a possible system oscillation due to feedback instability, the value of $\mathbf{R}_{xx}(0)$ also increases and therefore causes μ to decrease. It should also be noted that in the same algorithm, μ must not be allowed to be larger then μ_{max} in order to ensure that the stability region of the algorithm is not exceeded.

3.6 Combined Stability of the Control Algorithm

The control algorithm is based upon the LMS algorithm, but is more complex. To ensure system stability, and system identification, additional adaptive processes are added. As the number of channels increases, so does the number of simultaneous adaptive processes. Thus, stability of the control algorithm becomes a complicated issue to address.

As mentioned in section 3.2 of this thesis, Widrow *et al.* showed that convergence of the LMS algorithm is achieved if the convergence parameter is greater than zero, but less than the reciprocal value of the largest eignvalue of the autocorrelation matrix $\mathbf{R}_{xx}$. Assuming that $x(n)$ is a stationary process, the autocorrelation function of the input signal is given as follows:

$$R_{xx}(j-k) = E\{x(n-i-j)x(n-i-k)\}. \tag{3.20}$$

Thus, the maximum value of $R_{xx}(\tau)$ occurs for $R_{xx}(0)$, which corresponds to the average input signal power.

In the case of the filtered-x algorithm, the filtered version of the input signal is defined by

$$r_{lm}(n-i) \equiv \sum_{k=0}^{K-1} h_{lmk}(n)x(n-k-i), \tag{3.21}$$

and represented in vector form as

$$\begin{aligned} r_l^T(n) \equiv [&r_{l1}(n)\cdots r_{l1}(n-N+1) \vdots r_{l2}(n)\cdots r_{l2}(n-N+1) \vdots \\ &\cdots \vdots r_{lM}(n)\cdots r_{lM}(n-N+1)]. \end{aligned} \tag{3.22}$$

Using this in multichannel notation, let

$$R(n) \equiv [r_1(n)\ r_2(n)\cdots r_L(n)] \tag{3.23}$$

be the vector of the filtered output from all L sensors. Thus it can be shown [32] that

$$\begin{aligned} \lambda_{max} &\le trace\left[E\left\{R(n)R^T(n)\right\}\right] \\ &= trace\left[E\left\{\sum_{l=1}^{L} r_1(n)r_l^T(n)\right\}\right] \\ &= E\left\{\sum_{l=1}^{L}\sum_{m=1}^{M}\sum_{n'=1}^{N-1} r_{lm}^2(n-n')\right\}. \end{aligned} \tag{3.24}$$

Furthermore, using the definition of the filtered input signal, λ_{max} may be defined by

$$\lambda_{max} \leq \sum_{l=1}^{L} \sum_{m=1}^{M} \sum_{n'=0}^{N-1} \sum_{k=0}^{K-1} \sum_{j=0}^{K-1} h_{lmk}(n) h_{lmj}(n) R_{xx}(0). \tag{3.25}$$

Knowing the upper bound for $h_{lmk}(n)$, denoted as h_{max}, the value of the largest eignvalue can therefore be derived as

$$\lambda_{max} \leq h_{max}^2 [L \cdot M \cdot N \cdot K^2] R_{xx}(0). \tag{3.26}$$

This leads to an expression for a stable value of the convergence parameter, based on L error sensors, M control actuators, LMS filters of tap length N, and a projection algorithm of tap length K. The resulting convergence criterion is given by

$$0 < \mu < \frac{2}{h_{max}^2 [L \cdot M \cdot N \cdot K^2] R_{xx}(0)}. \tag{3.27}$$

Therefore, the adaptive μ algorithm is allowed to change the value for μ within this stable region.

When running a multichannel system, one must pay careful attention to the value of μ selected for each individual channel. If values chosen for each channel are very similar in value, convergence is not guaranteed. Such a situation causes a race condition in which one channel's convergence, when coupled through a mechanical system, causes another channel's divergence. As the other channel reconverges, it causes the first to diverge. If the convergence occurs at a constant rate for each channel, each channel will oscillate between convergence and divergence, with the result that the system does not globally converge for all of the channels. The value for μ_l is therefore selected as

follows:

$$\mu_l = \frac{\mu}{l^2} \tag{3.28}$$

where,

μ is based according to Equation (3.27)

$1 \leq l \leq L$.

3.7 Convergence of Combined Control Algorithm

The rate at which the algorithm converges is based heavily upon the value calculated for μ. However, since the system must be identified first, the projection algorithm is allowed to converge most rapidly. In order for convergence of the projection algorithm, its convergence parameter is chosen such that it converges at a faster rate than that of the LMS filter. Also, for the projection algorithm to identify the system, output from the LMS filter is required as input to the projection algorithm. It is therefore necessary to have two conditions. The first necessary condition is that several of the LMS filter's leading coefficients are set initially to a constant value, in order that an output signal is immediately produced. The second condition is that a ratio is established for the projection algorithm convergence rate to that of the LMS filter convergence rate. This ratio is denoted as β and is used to calculate a in equation (3.18). The convergence parameter μ is calculated for the LMS algorithm as follows:

$$\mu = \frac{2}{C\,[L \cdot M \cdot N \cdot K^2] R_{xx}(0)}, \tag{3.29}$$

where C is a constant which provides a conservative value for μ. The equivalent of the convergence parameter for the projection algorithm is seen in the leading fraction of equation (3.18). This leading fraction can be thought of as μ_{proj} and represented as

$$\begin{aligned} \mu_{proj} &\approx \frac{a}{KR_{xx}(0)+MKR_{yy}(0)} \\ &\approx \frac{a}{(M+1)KR_{xx}(0)} \end{aligned} \tag{3.30}$$

Defining a ratio of the projection algorithm convergence parameter to the LMS algorithm convergence parameter leads to a representation for β as

$$\beta = \frac{\mu_{proj}}{\mu_{LMS}} \approx \frac{[L \cdot M \cdot N \cdot K]\, a\, C}{2(M+1)}. \tag{3.31}$$

Thus choosing a ratio for β leads to a calculation for a in equation (3.18) as follows:

$$a = \frac{2\,\beta\,(M+1)}{[L \cdot M \cdot N \cdot K]\, C}. \tag{3.32}$$

Chapter 4

THE EXPERIMENTAL APPARATUS

The results described in this thesis were produced by an actual system. This system consisted of a mechanical system to which vibration control was applied, and an electronic system to perform the adaptive control. A description of both systems is presented in this chapter.

4.1 The Mechanical System

As mentioned in section 1.3, the mechanical system consisted of a rectangular metal plate, mounted to a rigid foundation with springs located near each of its four corners. Two plates were used in this thesis in order to study different effects of active control. The dimensions of both plates were sixteen by twenty-four inches. The first plate, made of aluminum, was one quarter of an inch thick, while the second plate, made of steel, was one sixteenth of an inch thick. The springs used in this study were produced by the Diamond Wire Spring Company and were rated at a spring constant of 15.8 pounds per inch. This gives an estimated lumped-mass resonance frequency of the aluminum and steel plate systems at 5.75 Hz and 9.62 Hz, respectively. These were

experimentally found to be approximately 9 Hz and 12 Hz, respectively.

Control for the plates was provided by four Wilcoxon Research F3 shakers. These shakers can be modelled as a lumped spring-mass system in the frequency range of interest, with the mass of each shaker rated at 0.7 lbs and a spring constant of about 87.9 lbs/inch. Each shaker is rated at 0.75 amps of continuous current, giving an acceptable dynamic range to the electronic controller. The F3 shaker is rated at having a useable frequency range from 30 to 40,000 Hz, with a resonance frequency at approximately 35 Hz. Low frequency response is slightly extended for the control system, due to the multiple number of shakers. These specifications provide excellent ranges in this active vibration control study.

The control shakers were attached near each of the corners of the plate, at a distance of one and a half inches from each side. The springs, as well as the error sensors, were attached three inches from each side, near each of the corners of the plate. As mentioned in chapter 2 of this thesis, completely free boundary conditions were used to solve for the resonance frequencies of the two plates used. In addition to the bending mode frequencies, the corresponding lumped-mass frequencies and control shaker resonance frequency must also be included in a broadband spectrum of the plate system.

Excitation to the plate was provided by a Wilcoxon Research F4 shaker, attached to the center of the plate. This shaker was rigidly attached to the foundation, and provided adequate force to excite the entire plate system. The F4 shaker is rated at having a useable frequency range from 25 to 40,000 Hz with a resonance frequency at 30 Hz.

4.2 The Electronic System

Adaptive control was achieved through the use of a Motorola DSP56000ADS development microprocessor. The DSP56000 is a high-speed microprocessor, dedicated to the use of digital signal processing. Its internal architecture allows the use of three memory banks, two for data processing, and a third for programming code. Additional features include parallel processing and a hardware DO loop feature which saves large amounts of time when writing algorithms. Motorola marketed this processor through a development system which included internal clocks and communication hardware, allowing easy interface to a host computer. In the case of this thesis, the host computer was an IBM AT and was used for software development, and monitoring of the stand-alone DSP56000 system.

Input and output of electronic analog signals was achieved through the use of an A/D D/A device, produced by the Ariel corporation. This product is the ADC56000 interface board, designed to directly interface with Motorola's DSP56000 development board. The ADC56000 board provides two channels of 16-bit data acquisition and can be "daisy-chained" with more ADC56000 boards to allow additional channels of input/output. Three such boards were used in this controller to provide one channel of input, four channels of error input, and four channels of control output. This also allowed one additional input, and two additional output channels, which proved effective for identifying problems with the control system.

For the case of feedback control, *a priori* compensation filters were used. These

filters were implemented through the use of stand-alone adaptive/fixed DSP56200 digital filter chips, produced by Motorola. Interface to the DSP56000 processor was accomplished through the 96-pin bus connector used by the Ariel ADC56000 boards. These filters were used in both their adaptive and fixed modes when used for feedback compensation of the system. These chips have several modes in which they can operate, and are easily controlled through a control register, which was written to through software commands.

Input to the electronic controller was provided by PCB piezoelectric accelerometers. These accelerometers convert vibrations into electrical signals which were then fed to the A/D converter boards of the control system. The particular model chosen for this experiment was the PCB 303A11 accelerometer, due to its high resolution and low mass. These accelerometers are accurate to 0.005 *g*, where one *g* corresponds to 32.2 ft/s^2. These accelerometers have an extremely flat frequency response from 10 to 10,000 Hz, and proved effective for measuring vibrations at the mounting points of the plate system, as well as vibrations at other locations of the plate. Attachment to the plate system was accomplished through the use of a convenient wax which is provided by PCB, and produces excellent results for low-frequency measurements.

Additional electronic hardware included anti-aliasing filters, small signal preamplifiers, charge amplifiers, and power amplifiers used to power the shakers.

Although most of the equipment used was purchased, some components such as the anti-aliasing filters and feedback control filters, were hand built. Algorithms for the control system were written in DSP56000 assembly language, so as to minimize the amount of code, and thus maximize the speed of the controller.

Chapter 5

EXPERIMENTAL RESULTS

Adaptive control has been studied considerably in theory and has recently been applied to different experimental problems. Results obtained from such experiments prove valuable as they can confirm theoretical predictions, and perhaps prove other predictions incorrect. Adaptive real-time control was applied to the experimental apparatus described in chapter 4 of this thesis, and provided informative results.

5.1 Effectiveness of 1- 2- and 4-Channel Control

The plate was mounted to springs at its four corners. The springs were mounted to a rigid foundation, resulting in four transmission paths to the foundation. The intent of this thesis was to minimize force transmission to the foundation. Since a rigid foundation is assumed, this corresponds to minimizing the vibration at the mounting locations. In order to achieve this vibration reduction, control actuators were attached near each corner and corresponding error sensors were attached at the mounting points of the springs. However, control was not applied to all of the corners in all cases. In developing the control algorithm, steps were taken to observe problems associated with

multichannel control. The result was the development of 1-, 2- and 4-channel versions of the control software. This allowed observation of both localized effects of adaptive control of a coupled system, and global effects of the control.

Sinusoidal waveforms were used to drive the plate into bending modes, thus creating vibrations with different phase relationships at the corners. Control was applied to the corners, and several effects were noticed. For Figures 5.1, 5.2, and 5.3, the thick aluminum plate was used and excited to its 3,1 mode at 170 Hz. Figure 5.1 shows the spectra of each of the corners with 1-channel control applied to the first corner. Solid lines indicate the spectra with control on and dashed lines indicate spectra with control off. Figures 5.2 and 5.3 show the same effective reduction for 2- and 4-channel control, respectively. The physical location was such that corners numbered 1 and 3 were diagonally opposed, as were corners numbered 2 and 4. It should also be noted that for calibration purposes, the vertical scales of the spectra are in dBV, meaning 20 times the log of the root-mean-square (rms) amplitude in volts, referenced to 1 volt. The voltage sensitivity of the accelerometers used was approximately 100 *mV/g* and the resolution of the accelerometers was .005 *g*. Also, preamplifiers were used with a total gain of approximately 39 dB.

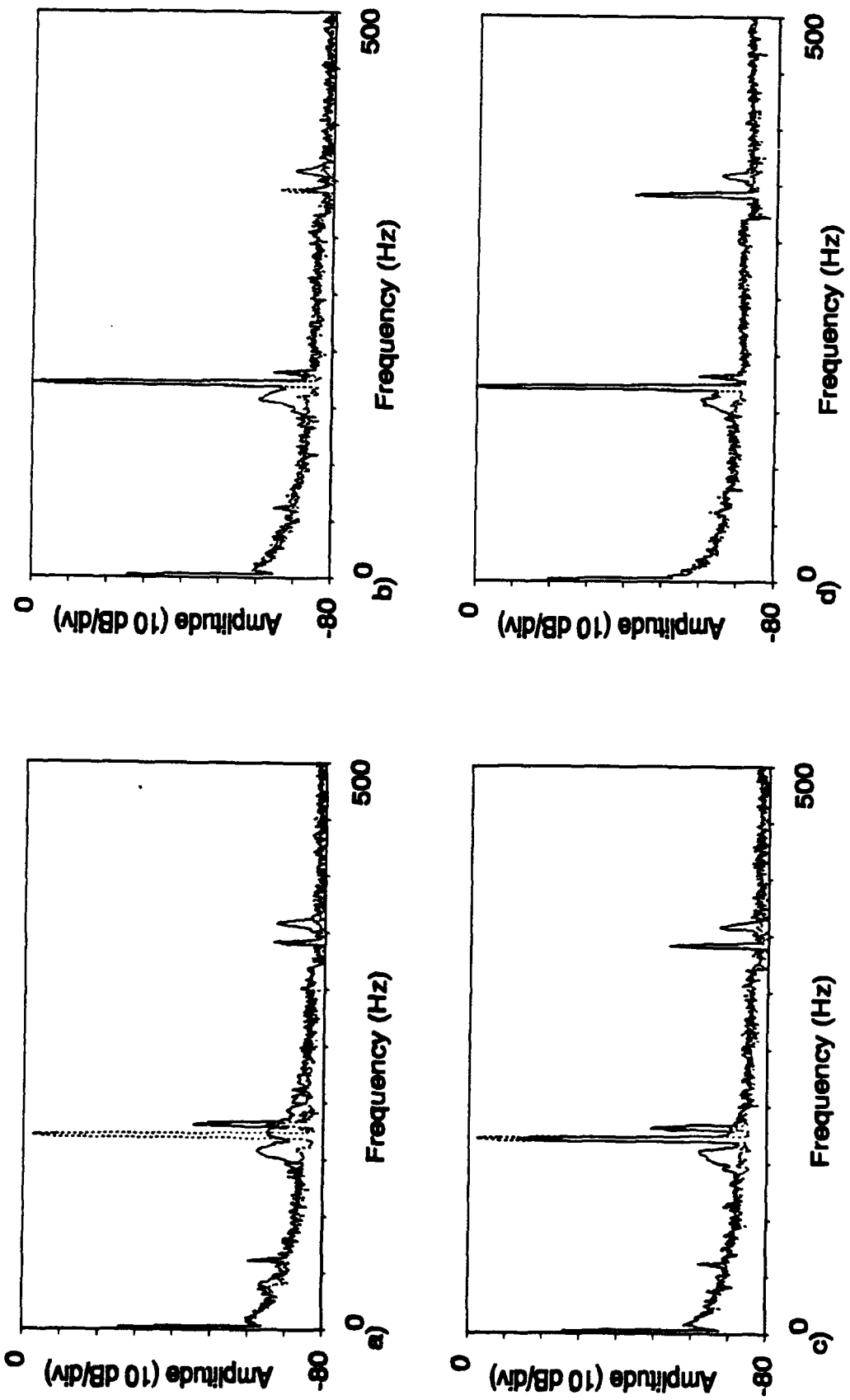

Figure 5.1: One-channel control applied at corner # 1. a) Corner #1. b) Corner #2. c) Corner #3. d) Corner #4.

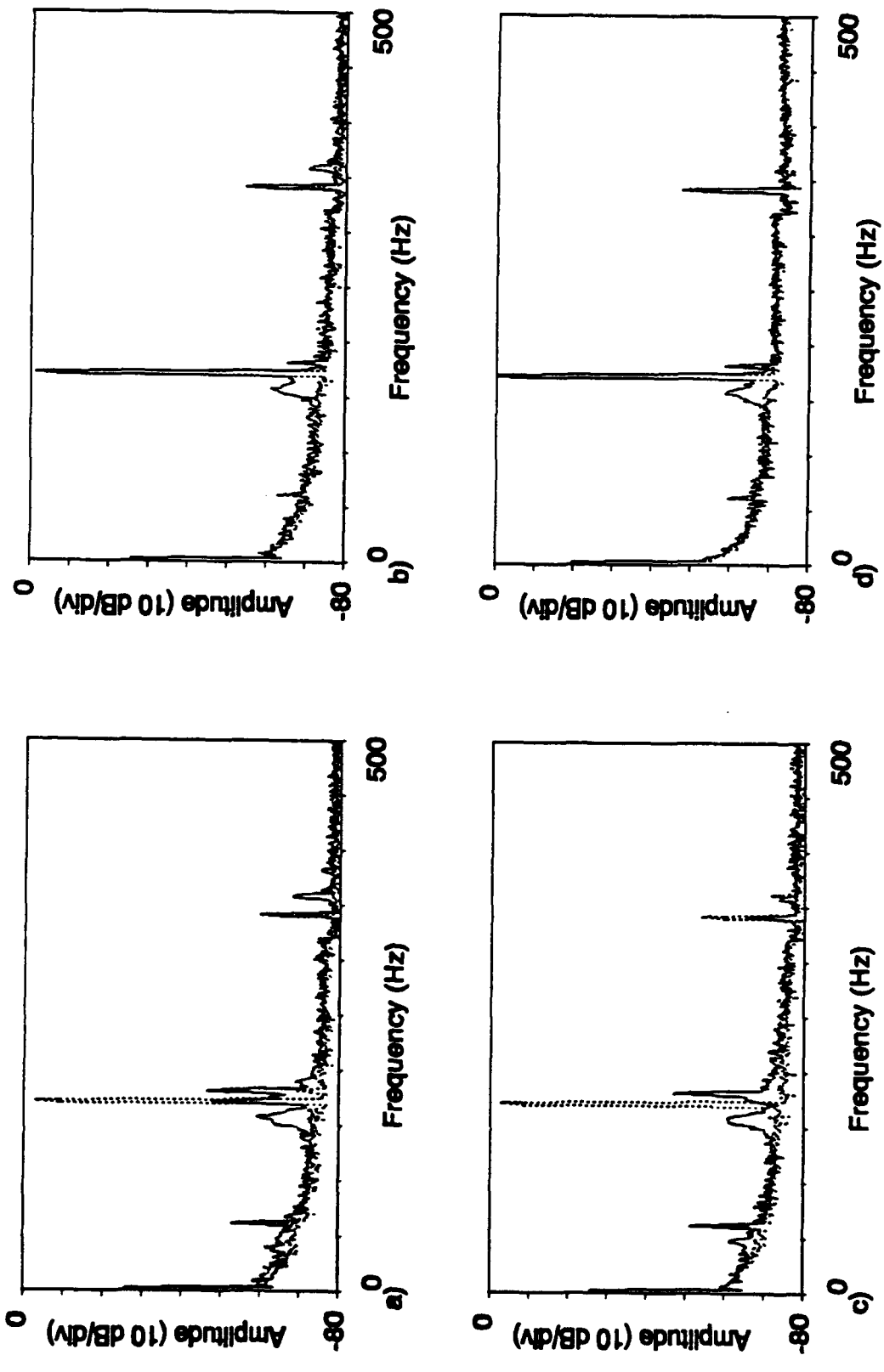

Figure 5.2: Two-channel control applied at corner #1 and corner #3. a) Corner #1. b) Corner #2. c) Corner #3. d) Corner #4.

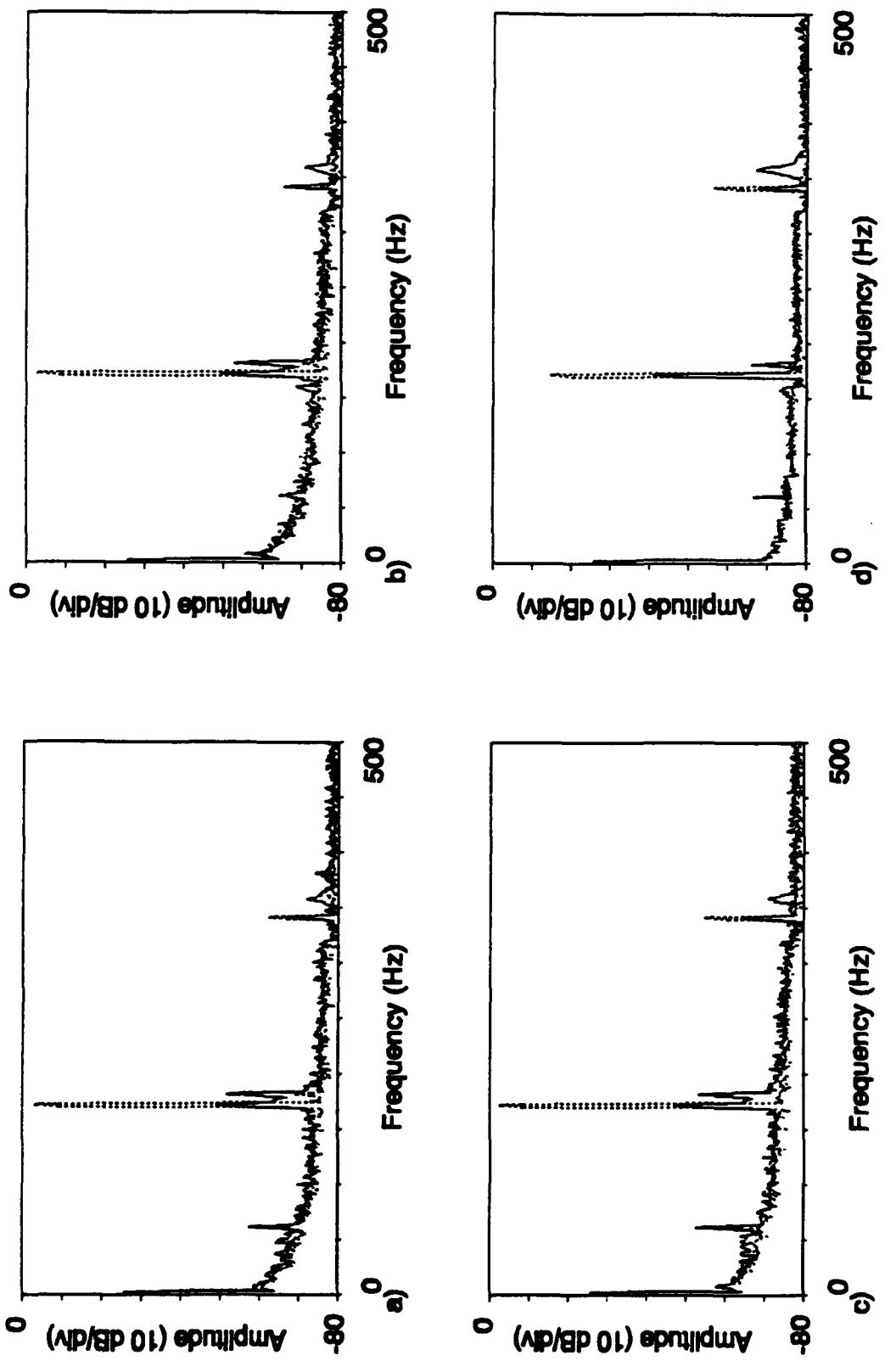

Figure 5.3: Four-channel control applied at all corners. a) Corner #1. b) Corner #2. c) Corner #3. d) Corner #4.

As seen in the previous figures, the localized effects of active control can be observed. Such control was capable of reducing vibrations at the transmission paths by approximately 70 dB, in some cases. Also, in order for all four transmission paths to be attenuated, all four corners had to be actively controlled, and thus had certain drawbacks. Since there are multiple adaptive processes running simultaneously, slower convergence times must be expected. As seen in Figures 5.4, 5.5, and 5.6 convergence occurs at a slower rate as the number of channels increases for 1-, 2- and 4-channel control, respectively.

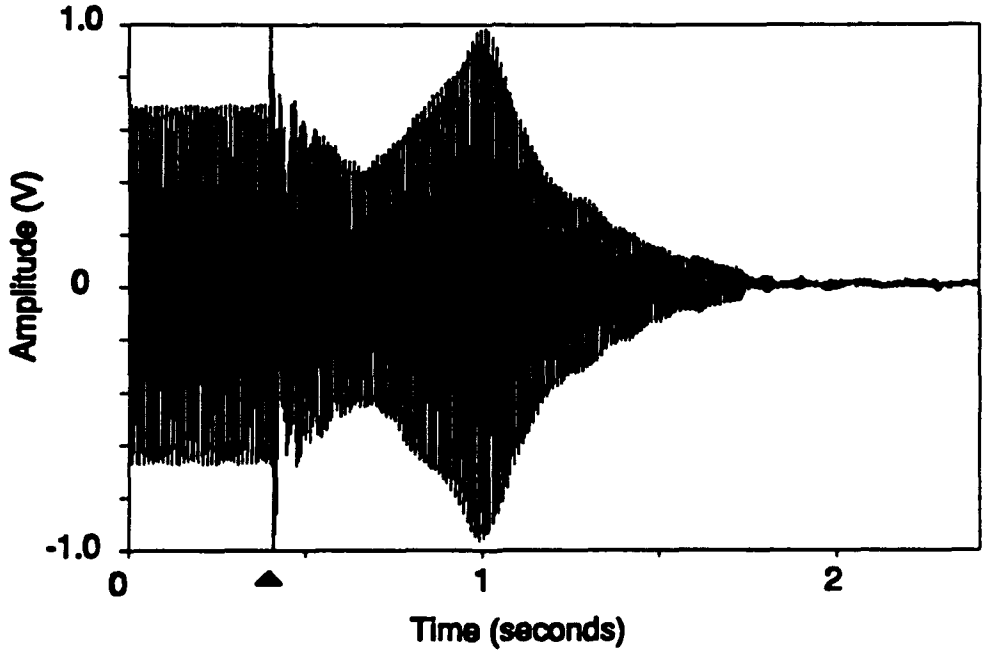

Figure 5.4: Convergence time of one-channel control

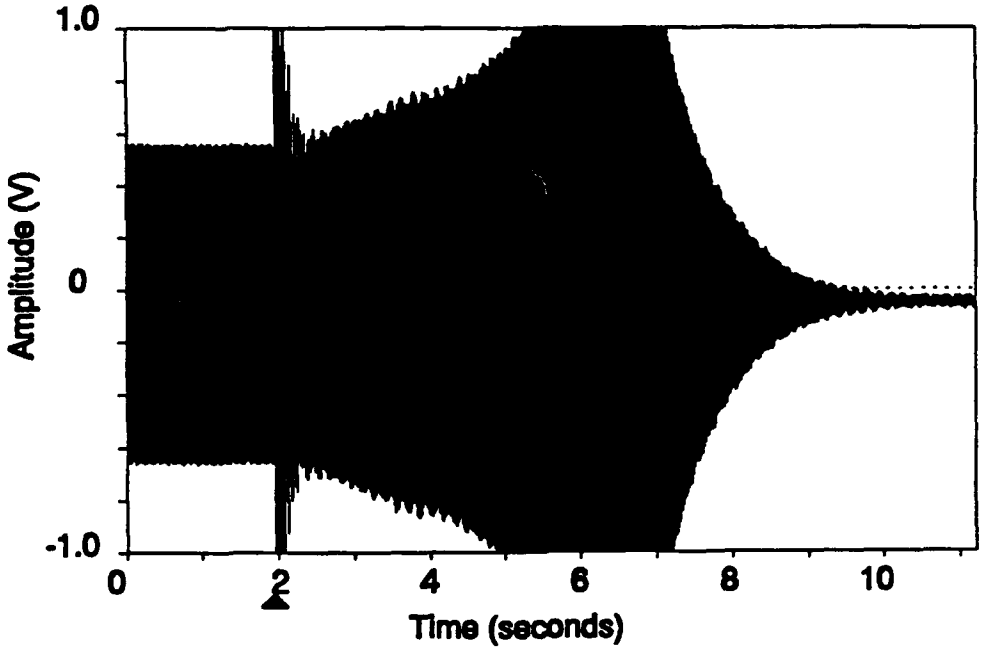

Figure 5.5: Convergence time of two-channel control

It should be noted that the arrow located on the time axis represents the time the algorithm began execution. The effects of such a study show that 2-channel control takes approximately four times as long to converge when compared to 1-channel control, and that 4-channel control takes approximately sixteen times as long to converge. Such convergence times are an important issue to consider for a particular application.

All of the previous data was for a single sinusoid exciting a single mode. The mode notation used in this thesis describes the m,n mode, where m-1 corresponds to the number of nodal lines in the x-direction, and n-1 corresponds to the number of nodal lines in the y-direction of the plate. In the previous data, the 3,1 mode was excited, producing similar phase relationships along the opposite edges of the y-direction of the plate. If the

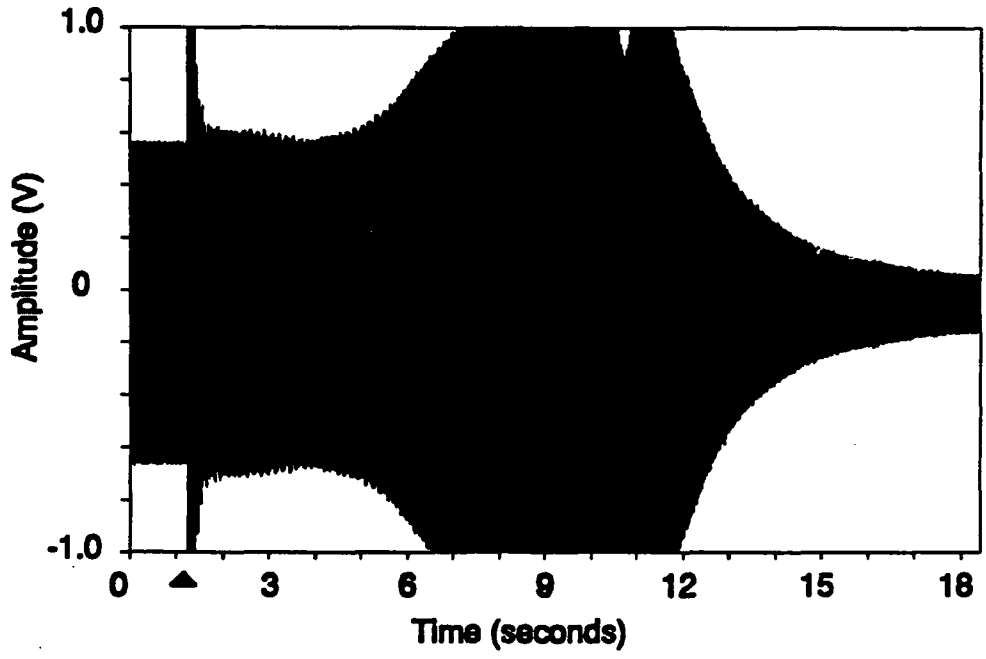

Figure 5.6: Convergence time of four-channel control

1,3 mode was excited, similar phase would exist along the x-direction of the plate. Realistic applications seldom consist of a single frequency excitation. Therefore, the controller was tested for multiple frequency excitation. In this test, the aluminum plate was simultaneously excited to its 3,1 mode and 1,3 mode at 170 Hz and 380 Hz, respectively. In this case, the controller had to match the appropriate phase and magnitude characteristics at multiple frequencies, and thus provided an excellent experiment for testing the effects of multichannel control. In Figures 5.7 and 5.8, the ability of the controller to attenuate 2 resonances simultaneously is shown. The corners represented in these figures are the same points where 2-channel control was applied. From this experiment it was seen that 4-channel control provided better attenuation than

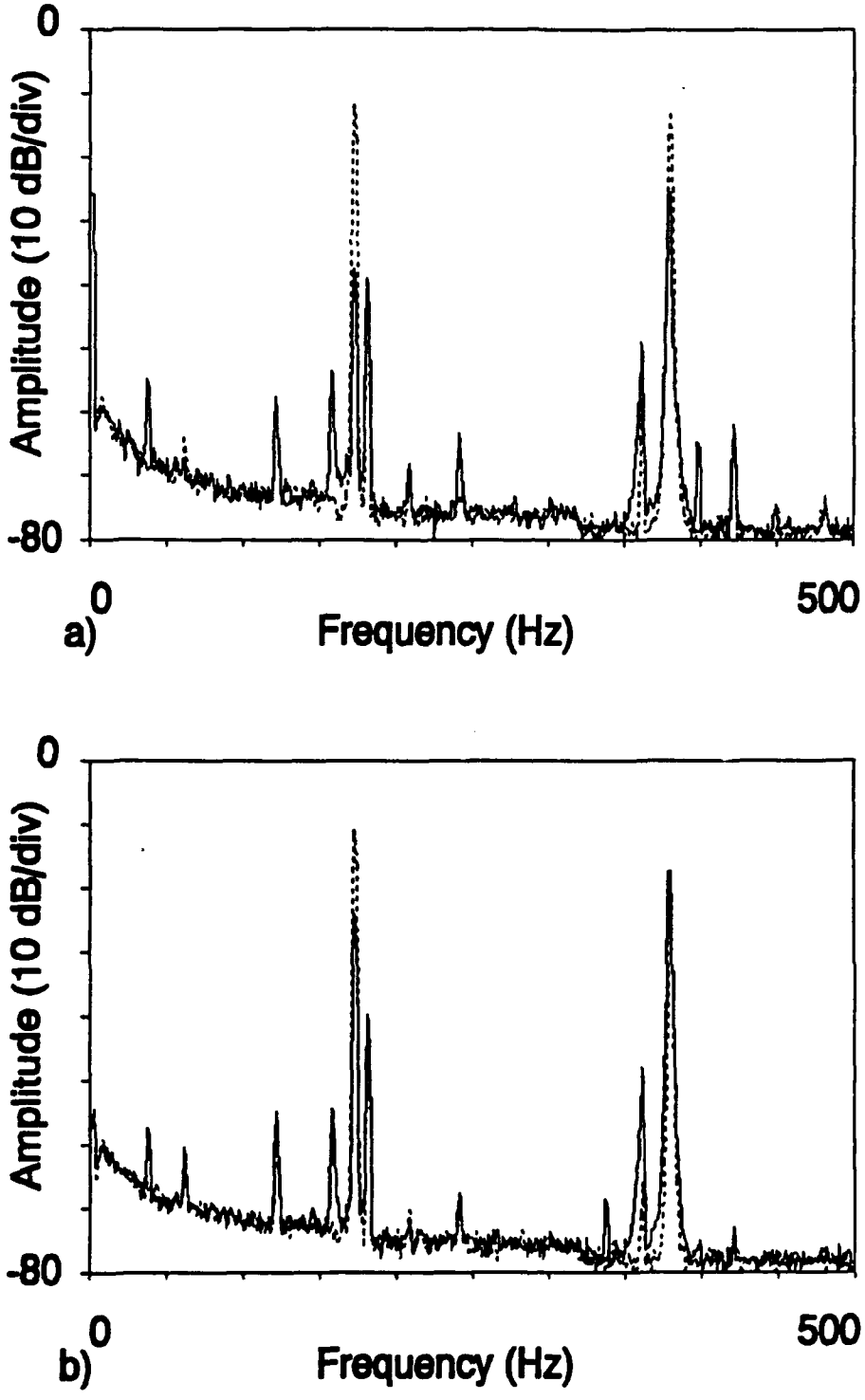

Figure 5.7: Two-channel control of 2 resonances. a) Corner #1. b) Corner #3.

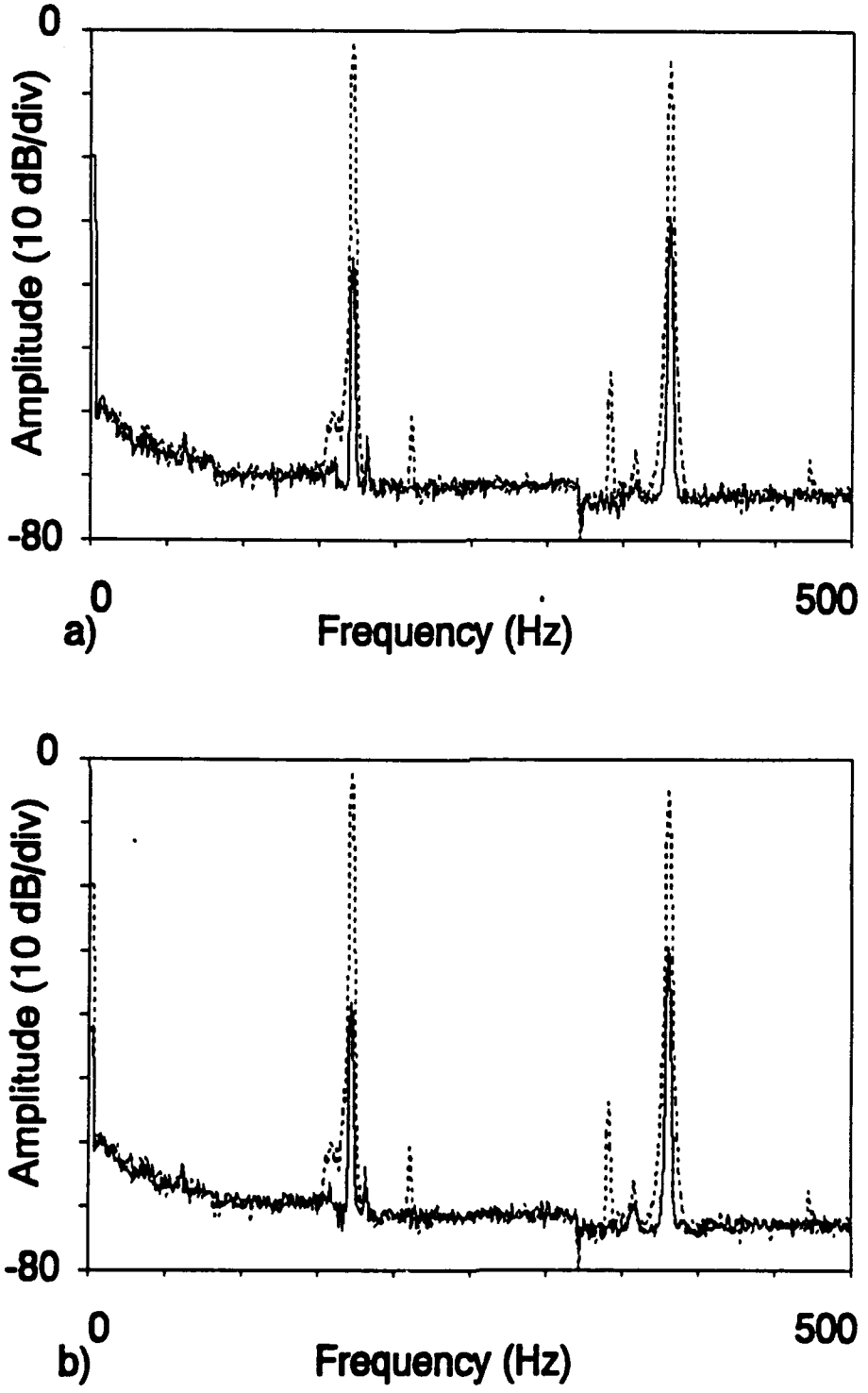

Figure 5.8: Four-channel control of 2 resonances. a) Corner #1. b) Corner #3.

2-channel control at the same points. This demonstrated that the controller could more effectively reduce multiple frequency vibrations when the number of control channels was increased. This was not the case for the 3,1 mode excitation, which only involved a single frequency.

5.2 Effectiveness of Feedback Compensation

The previous data was obtained using a reference signal derived from the noise source directly. In many practical situations, it may be necessary to obtain this signal from a measurement near a noise source driving point. Associated with this type of experiment is the problem of feedback from the control sources to the input sensor, which must be properly compensated for in order to maintain system stability.

This experiment was tested using *a priori* feedback compensation filters as described in section 3.4 of this thesis. It should be noted that due to system limitations, only 2-channel feedback compensation could be tested. Figure 5.9 shows the effective reduction using feedback compensation. When compared to Figure 5.2, essentially identical performance of the controller was observed showing that the *a priori* filters accurately accounted for the feedback through the system.

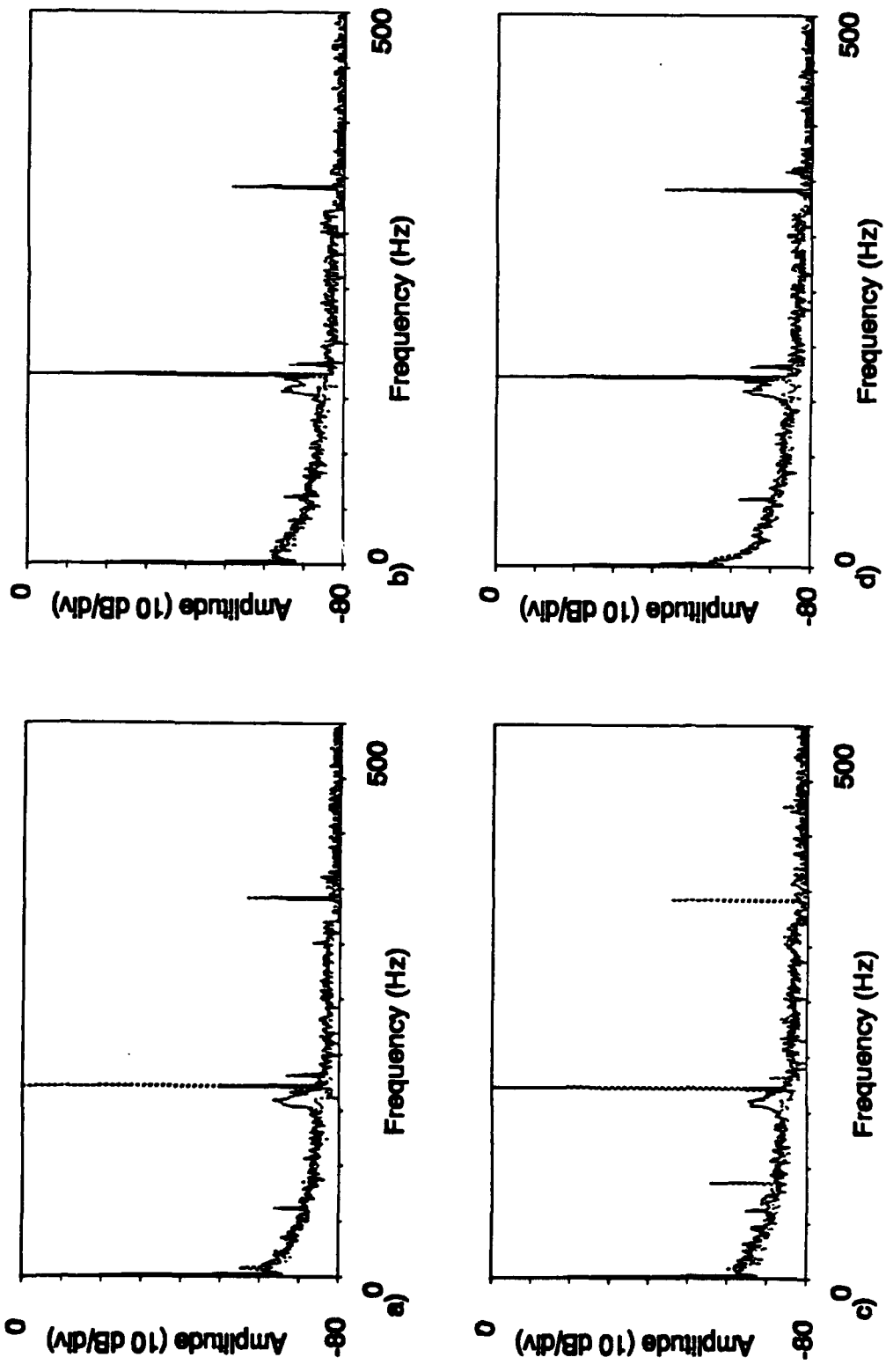

Figure 5.9: Feedback compensated two-channel control applied to corner #1 and corner #3. a) Corner #1. b) Corner #2. c) Corner #3. d) Corner #4.

5.3 Effects on Modal Patterns

The previous sections of this chapter dealt with the localized effects of the control at the transmission paths. The intent of this experiment was to minimize transmission to the foundation by adaptive control, and as demonstrated, was effective in doing so. One interesting effect that was also studied in this test was that of adaptive control on the modal patterns of the vibrating plate. This study provides an interesting prelude to such topics as ideal control actuator/sensor location, modal shifting, localized versus global effects of vibration control, and simple boundary condition changes caused by inactive control actuators.

In order to study the modal patterns, careful amplitude and phase measurements were made with respect to the noise source driving point of the plate. This data was then used in graphics generation software to provide the 3-dimensional and contour plots presented in this section of the thesis. The first modal pattern observed was the 3,1 mode of the thick aluminum plate. Figures 5.10 and 5.11 show the amplitudes of the vibrations at 2-inch increments across the surface of the plate, in contour and 3-dimensional representation, respectively. The contour and 3-dimensional plots are in dB, referenced to the driving point, i.e. the center of the plate.

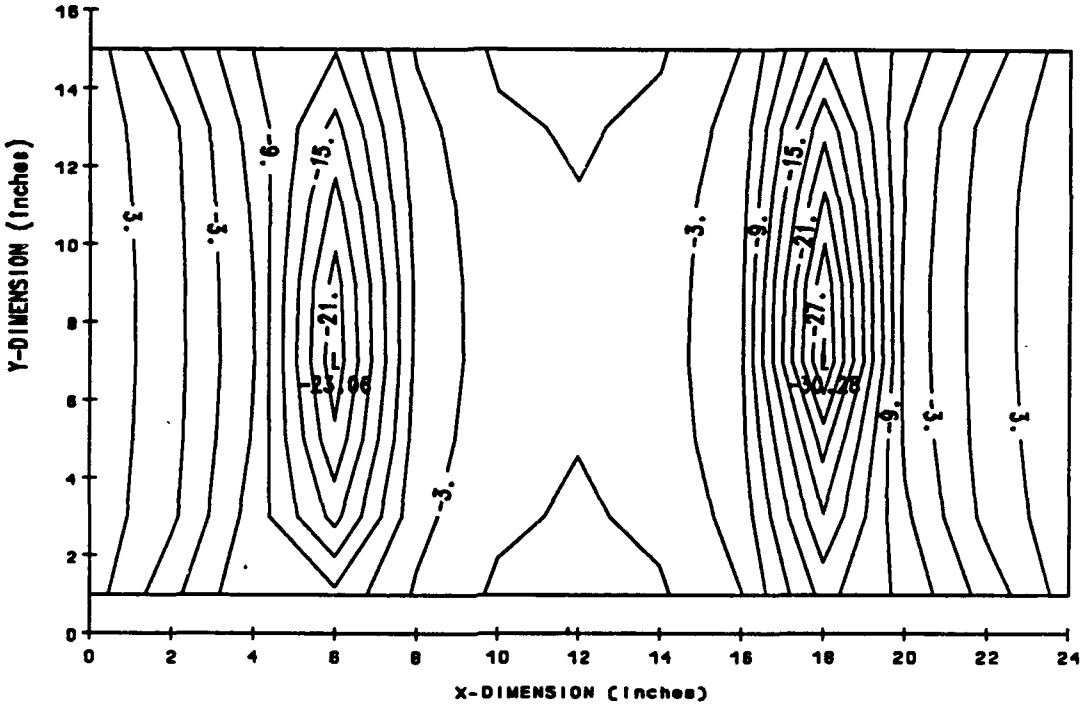

Figure 5.10: Contour plot of 3,1 mode

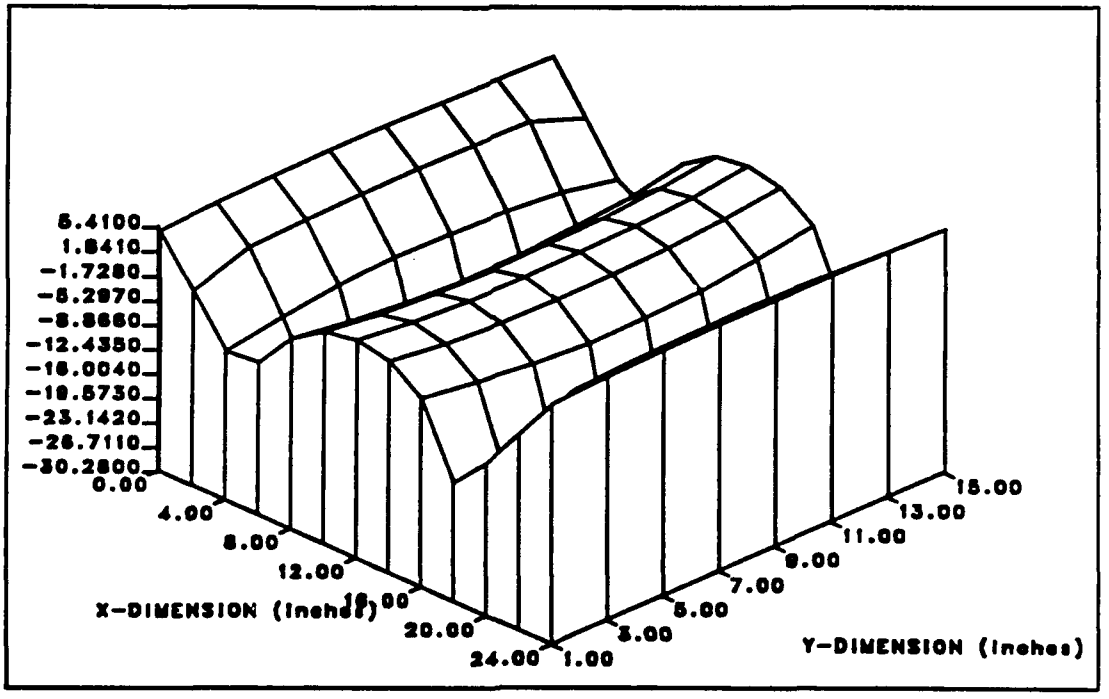

Figure 5.11: Three-dimensional plot of 3,1 mode

From Figures 5.10 and 5.11 and the knowledge that the error sensors are located at a distance of three inches from each corner, effective control is expected, due to the fact that the error sensors are not physically near nodal lines. Adaptive control was applied to this mode, and the results from this experiment are shown on the following pages. Figures 5.12 and 5.13 show the amplitudes of vibrations for 2-channel control. Since the error sensors imposed point constraints on the vibrating plate, when control was activated, one can see the bending of the nodal lines towards the error sensors. The effective reduction is shown in Figures 5.14 and 5.15. In the reduction plots, negative values correspond to a reduction in vibration amplitude.

Similar results for 4-channel control are shown in Figures 5.16 through 5.19. In this case, a more uniformly distributed reduction is shown. Also noticed, were the effects of control near nodal lines. Such nodal lines were shown to have small amplitude vibrations without control, and thus the controller was not able to provide much reduction near these nodal lines. Hence the effect of 4-channel control is to greatly decrease the displacement amplitudes near antinodes, but not greatly affect nodal lines, which are low in amplitude to begin with.

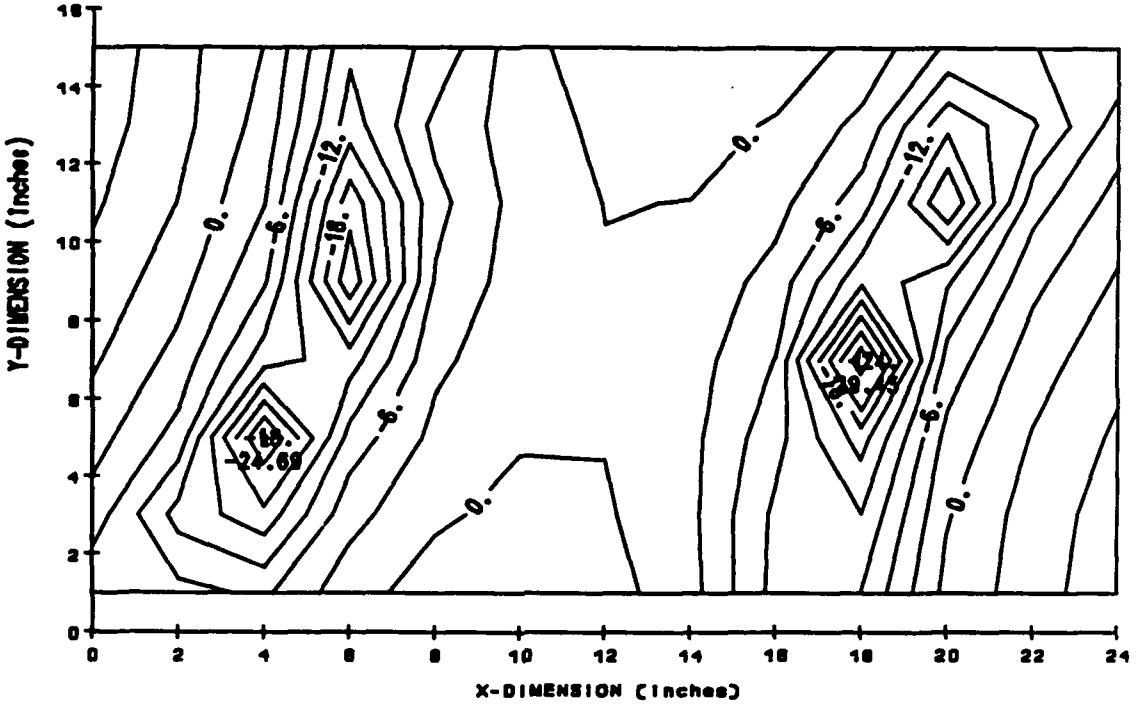

Figure 5.12: Contour plot of two-channel control of 3,1 mode

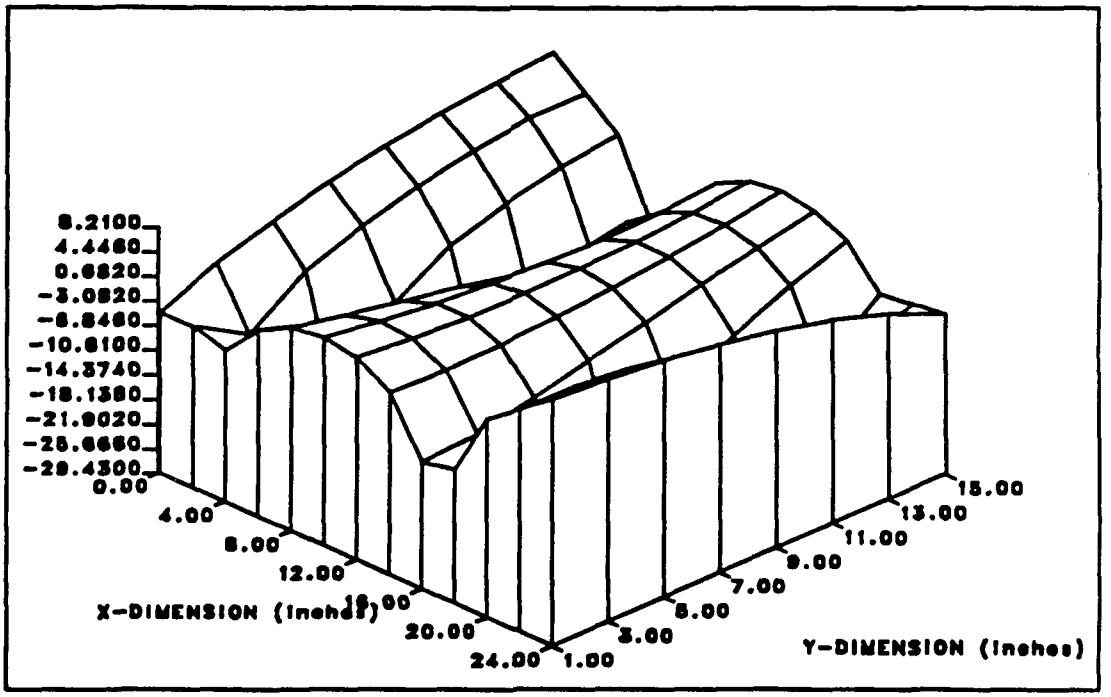

Figure 5.13: Three-dimensional plot of two-channel control of 3,1 mode

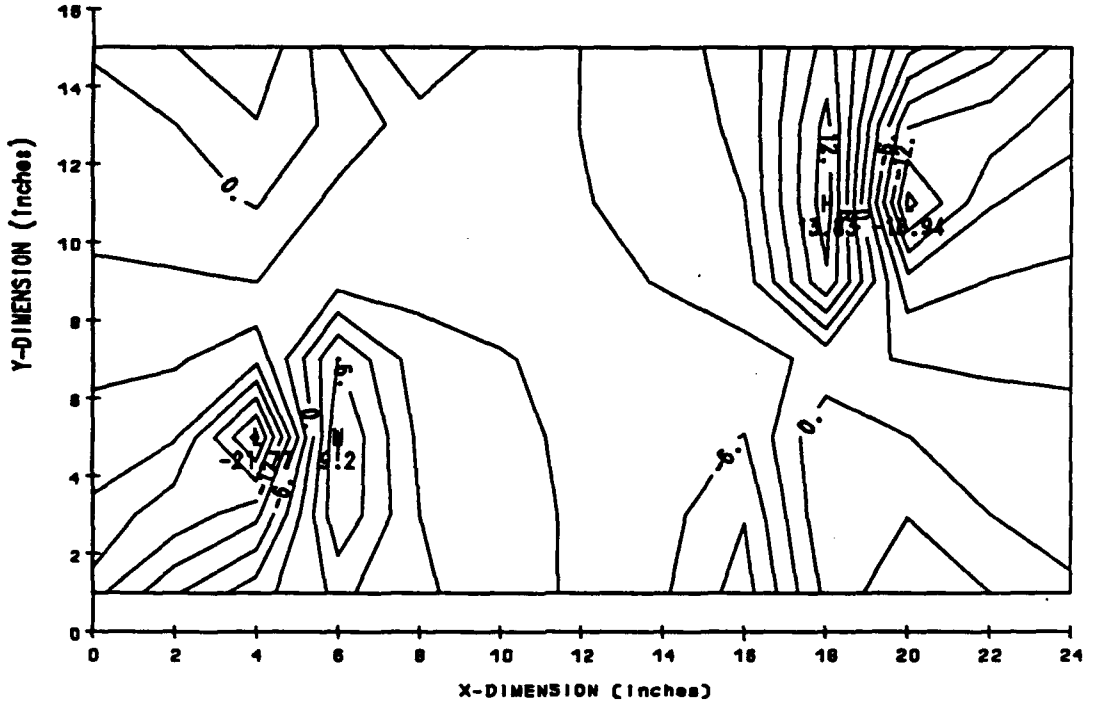

Figure 5.14: Contour plot of two-channel reduction of 3,1 mode

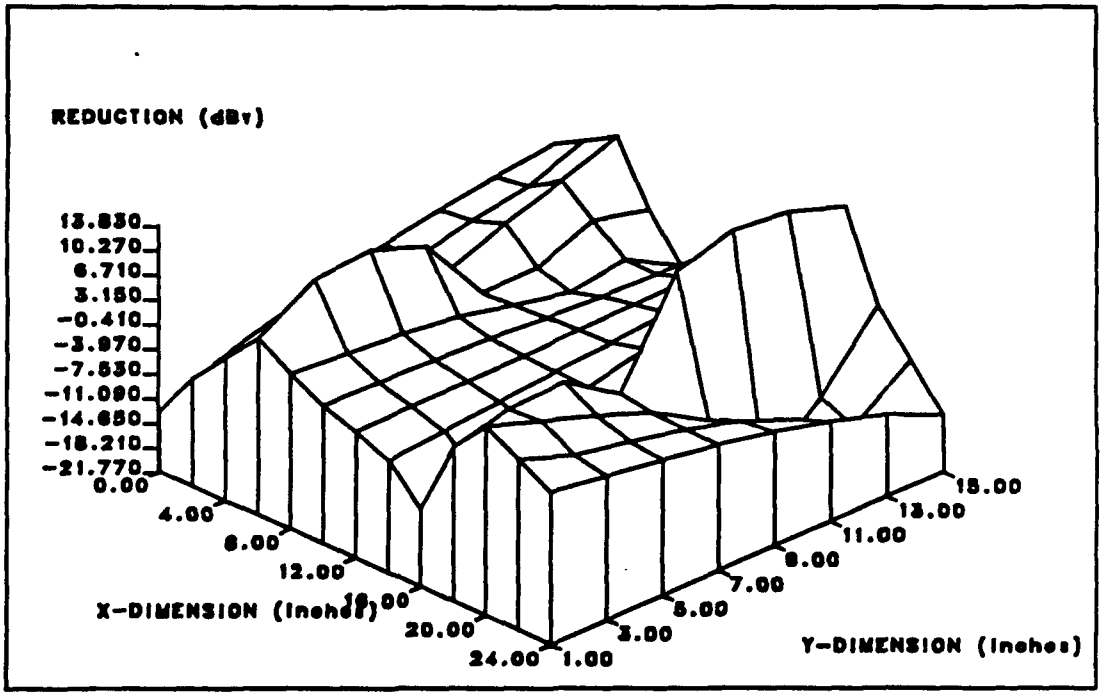

Figure 5.15: Three-dimensional plot of two-channel reduction of 3,1 mode

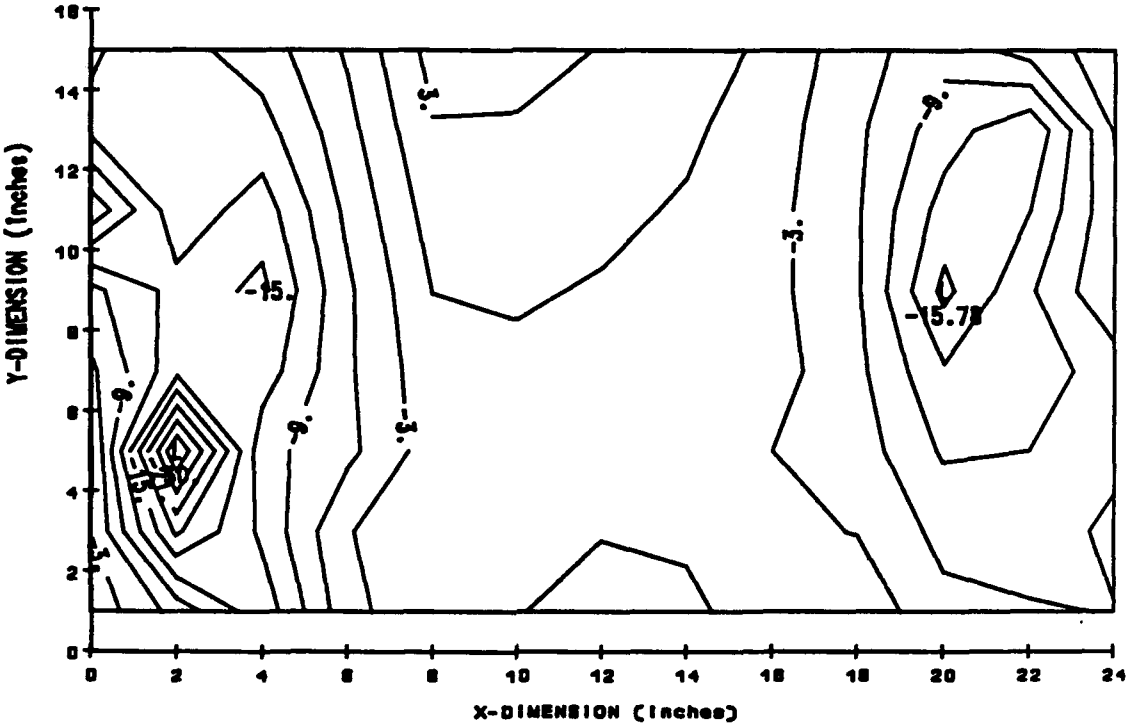

Figure 5.16: Contour plot of four-channel control of 3,1 mode

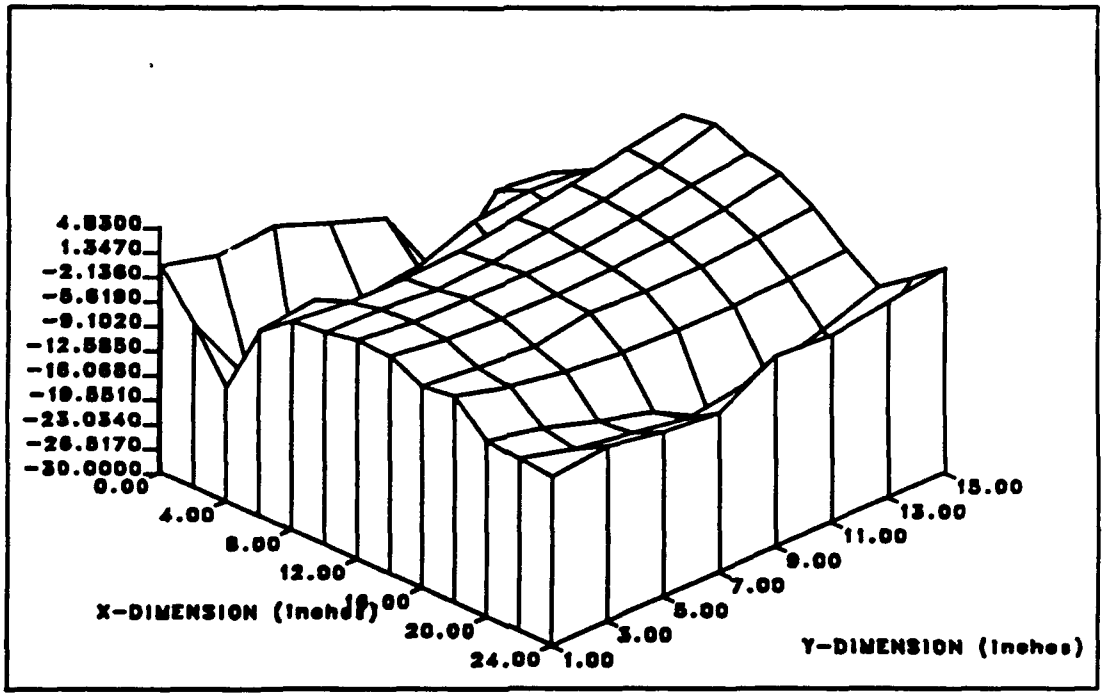

Figure 5.17: Three-dimensional plot of four-channel control of 3,1 mode

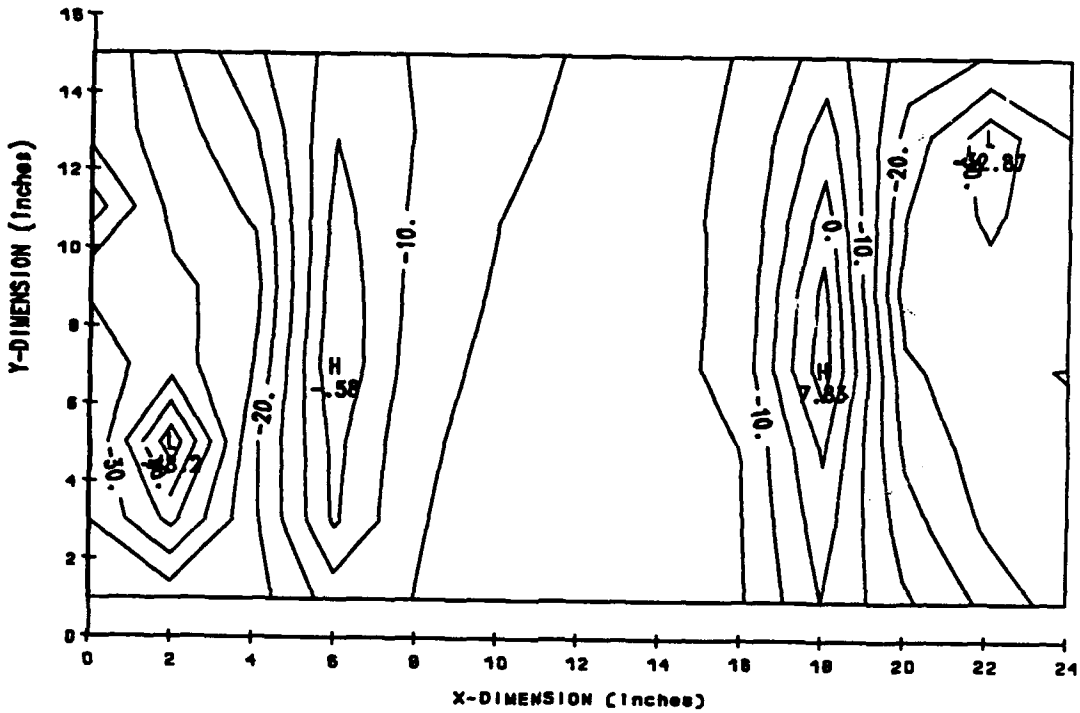

Figure 5.18: Contour plot of four-channel reduction of 3,1 mode

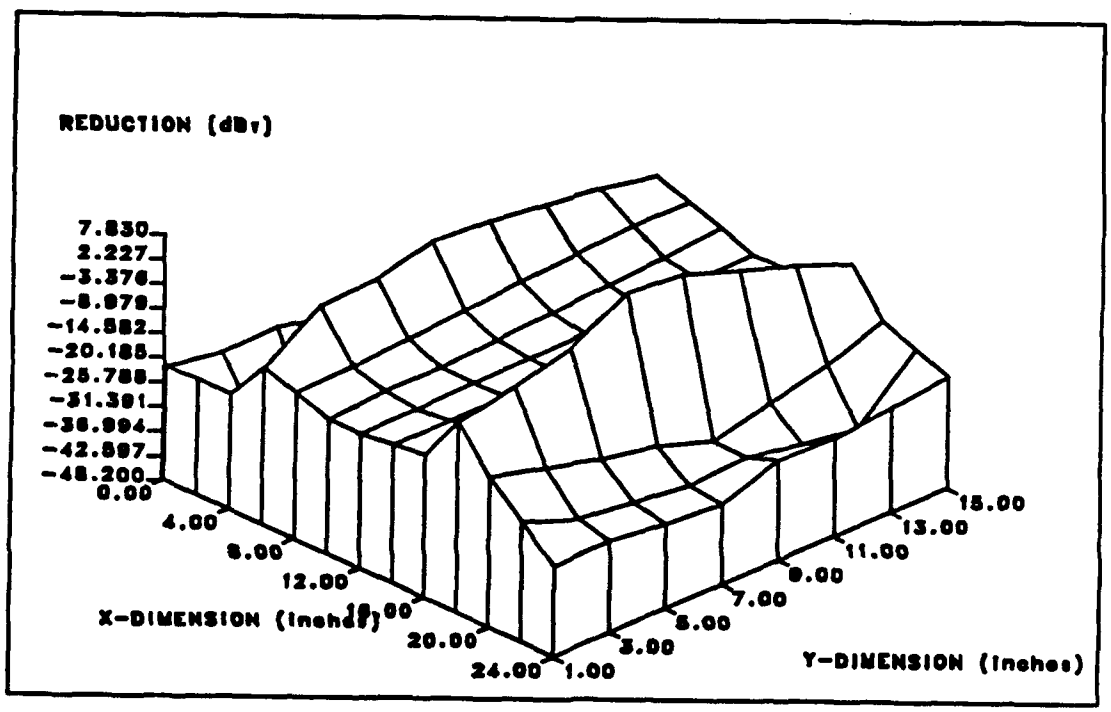

Figure 5.19: Three-dimensional plot of four-channel reduction of 3,1 mode

Another interesting experiment showed the effect of active control when error sensors are located near nodal lines. To demonstrate this, the aluminum plate was excited in its 1,3 mode at 380 Hz. The free vibrations of this mode are shown in Figures 5.20 and 5.21. When this mode was excited, two nodal lines appeared running lengthwise in the X-direction of the plate. These nodal lines were spaced such that they intercepted the location of the error sensors. This posed an interesting problem for the controller, as the error sensors were already measuring a small amplitude vibration before the algorithm was executed. When 2-channel control was applied, the modal pattern appeared to be relatively unaffected. In fact, the reduction appeared to be almost uniform across the entire surface of the plate, but not as locally effective as that in the 3,1 mode. Vibration patterns and reduction plots can be seen in Figures 5.22 through 5.25. This shows that in order for active control to be locally effective, and change the modal patterns significantly, error sensors should be located near antinodes. For a more global cancellation, error sensors may be located near nodes, with a lesser degree of performance from the algorithm and thus less localized reduction, but a relatively unaffected modal pattern.

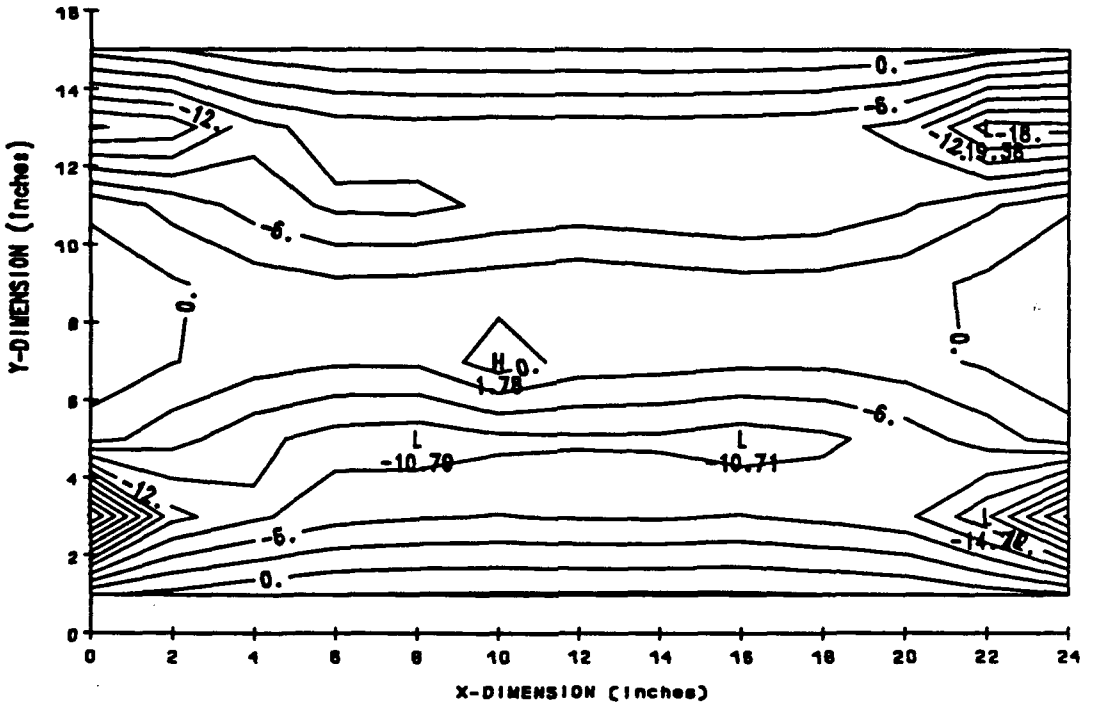

Figure 5.20: Contour plot of 1,3 mode

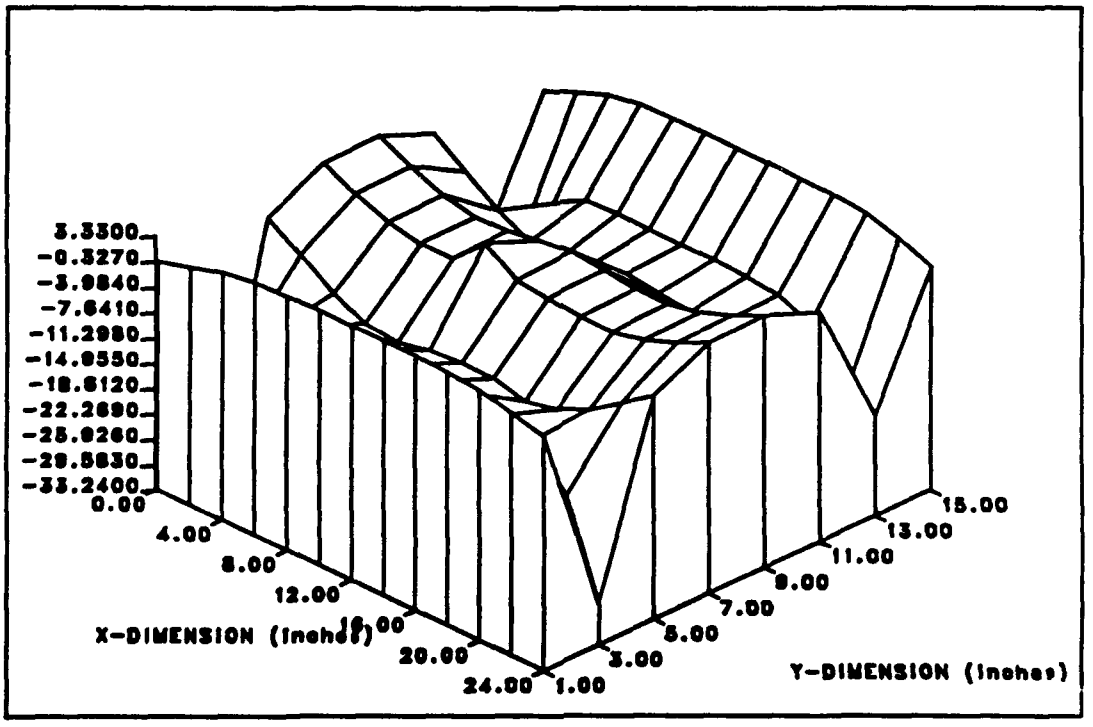

Figure 5.21: Three-dimensional plot of 1,3 mode

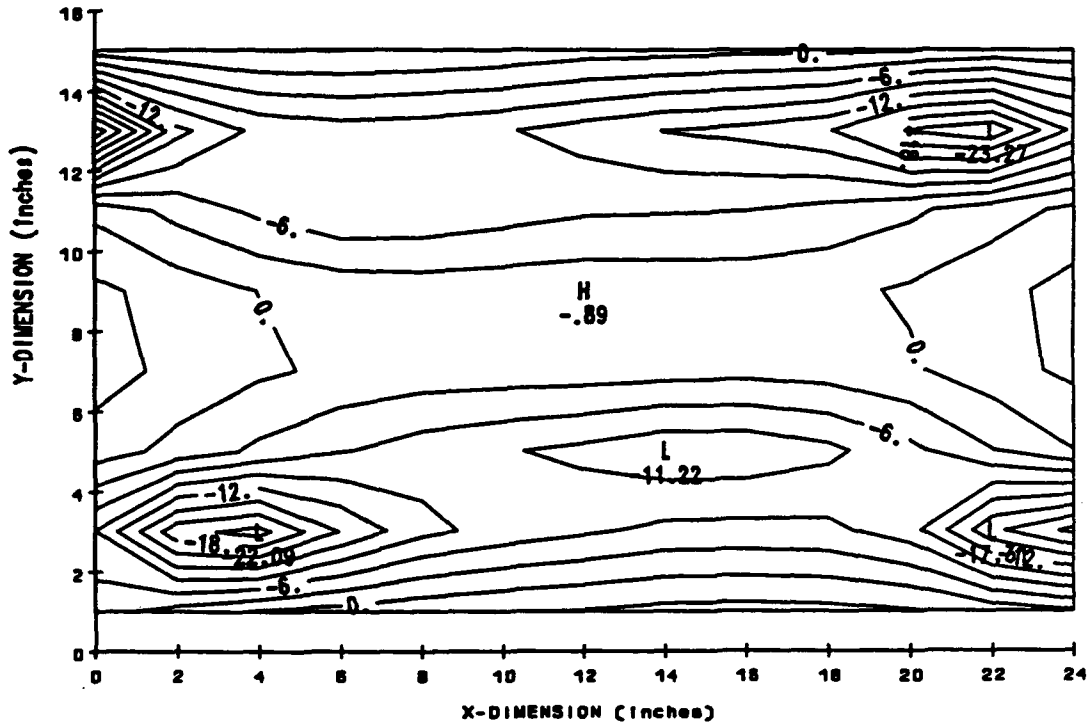

Figure 5.22: Contour plot of two-channel control of 1,3 mode

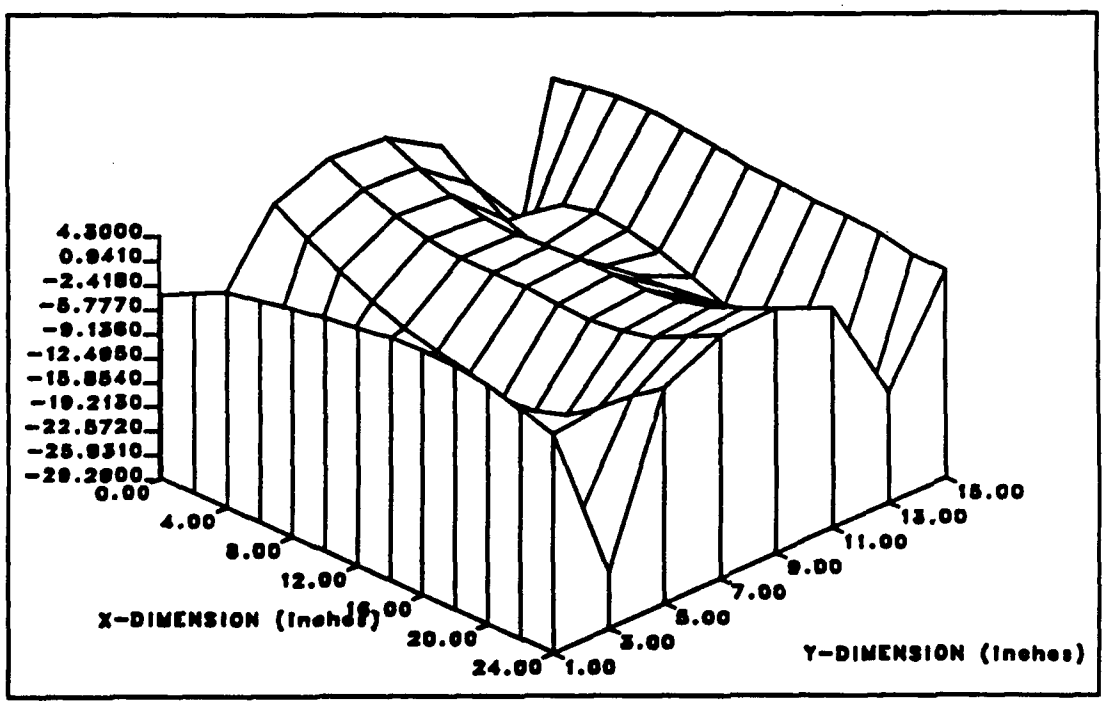

Figure 5.23: Three-dimensional plot of two-channel control of 1,3 mode

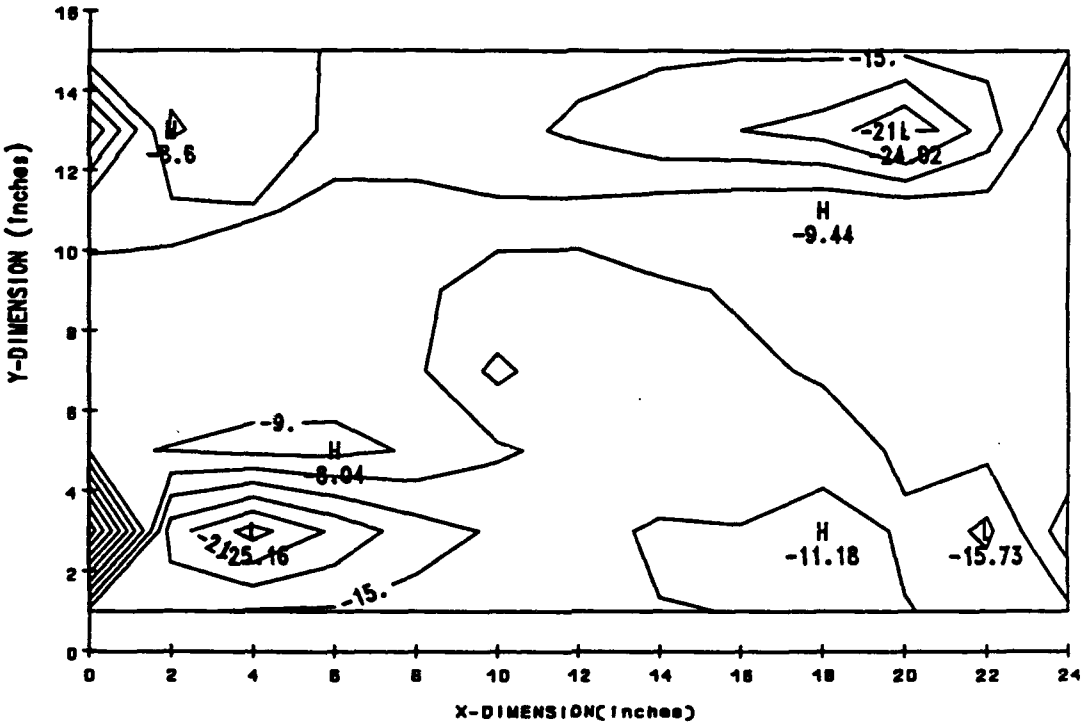

Figure 5.24: Contour plot of two-channel reduction of 1,3 mode

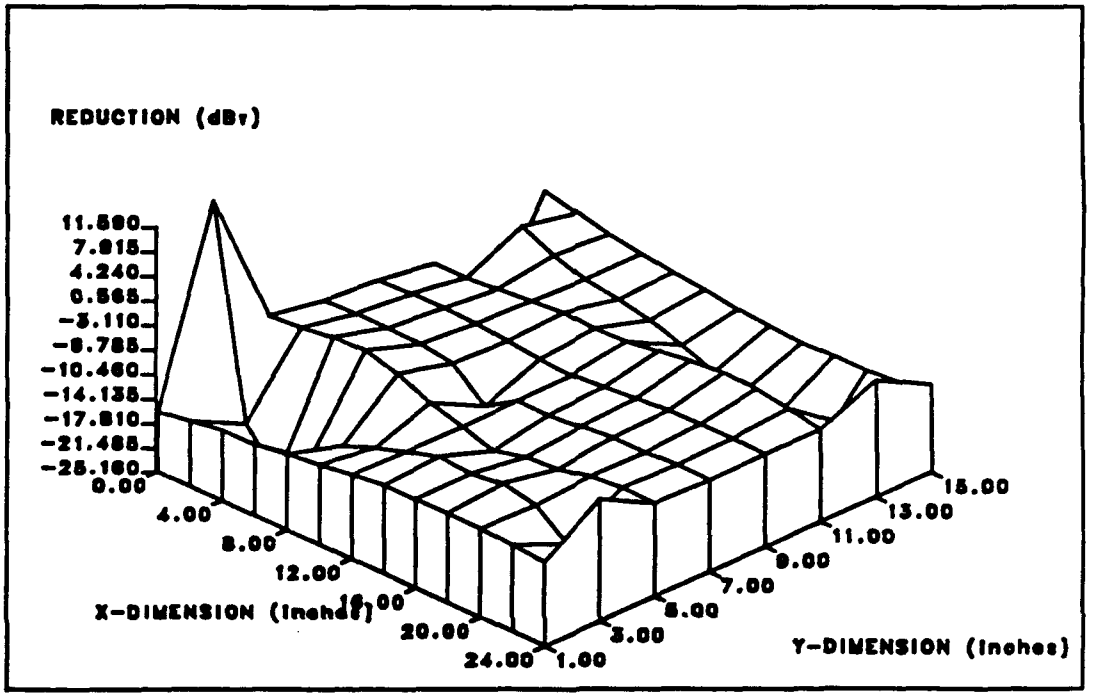

Figure 5.25: Three-dimensional plot of two-channel reduction of 1,3 mode

Previous modal analysis plots were obtained using the thick aluminum plate described in earlier sections of this thesis. Due to the large mass of this plate, changes in boundary conditions due to inactive control actuators did not significantly affect the vibration patterns of the plate. When the thin, more flexible plate was used, interesting effects were observed.

The first observation was that experimentally measured resonance frequencies did not correspond with values predicted in chapter 2 of this thesis. Resonance frequencies were measured at higher values than the frequencies predicted by Leissa's tables [33] for a completely free plate, indicating that the additional mass of the shakers was not causing simple mass loading of the plate. The inactive shakers were causing point constraints near the corners, thereby significantly altering the mode shapes and shifting the resonance frequencies of the lower order modes to higher frequencies. When the control actuators were removed, resonance frequencies occurred near the predicted values. Values recorded in Table 2.2 were measured with the shakers removed. Therefore, a shift in the lower resonance frequencies had to be approximated in order to predict where resonance frequencies would occur with the control actuators attached to the plate system. At higher frequencies, more wavelengths are distributed across the plate, and therefore, the higher resonance frequencies are affected to a lesser degree.

The thin plate was originally intended for observation of control on a system with more modes in the frequency range of the controller. Also, due to a higher modal overlap, coupling of modes was a topic that was experimented with. Such modal coupling was observed when excitation of the 4,1 mode was attempted. As seen in Table

2.2, the 4,1 and 1,3 modes were only separated by a predicted value of approximately 8.2 Hz. Figures 5.26 and 5.27 show the contribution of both the 1,3 and 4,1 modes on the vibration pattern of the thin plate when the driving frequency was set at 60.5 Hz. The modal measurements at this frequency were made with the shakers removed from the corners.

The boundary condition effects due to the inactive control shakers did provide some reduction in the displacement amplitude of vibrations measured near the corners. Figures 5.28 and 5.29 show the vibration patterns of the thin plate at the 3,2 mode with the shakers removed. Figures 5.30 and 5.31 show the same effective mode with the shakers attached at the corners. As seen, the vibrations measured at the corners were reduced, and thus made it difficult at times to determine the mode at which the plate was vibrating. The corresponding resonance frequencies occurred at 47.5 Hz without the shakers attached, and 112 Hz with the shakers attached. Thus, the resonance frequency shift was 64.5 Hz, showing that it was no longer valid to assume completely free boundary conditions.

Similar effects to that of the aluminum plate were noticed when control was applied. Although the imposed constraints, due to the inactive control shakers, reduced the amplitude of vibrations at the corners, the error sensors were still located near antinodes, and thus the controller provided effective reduction. Figures 5.32 through 5.35 show the vibration patterns and corresponding reduction for 4-channel control. A change in modal patterns was recognizable as the controller appeared to force the plate into a 3,3 mode with localized reduction at the corners.

Similar modal shifting was apparent when 4-channel control of the effective 2,2 mode was attempted. In this experiment, the thin plate was excited to its effective 2,2 mode, and both 2- and 4-channel control were performed. For the case of 2-channel control, localized reduction resulted, producing a line of reduced amplitude vibrations intercepting both of the control actuators and error sensors. In the case of 4-channel control, the plate appeared to be forced into an effective 3,3 mode with large reduction across most of the surface of the plate. Figures 5.36 through 5.45 show the results of the effective 2,2 mode of the thin plate.

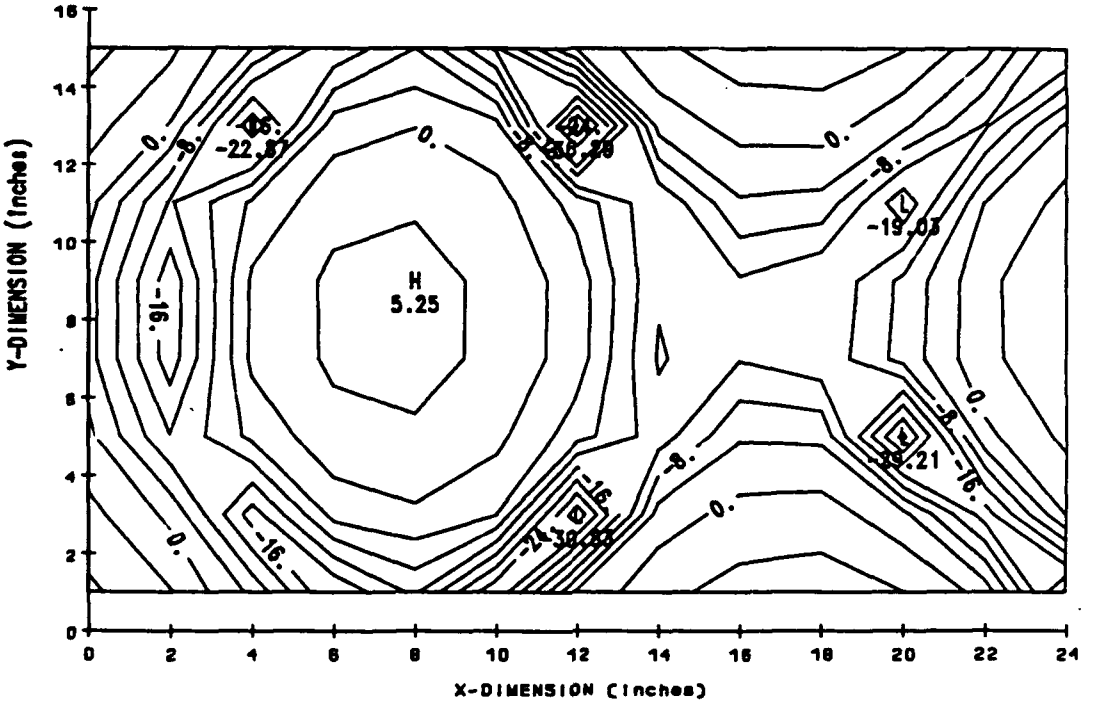

Figure 5.26: Contour plot of 1,3 and 4,1 modes excited by a 60.5 Hz signal

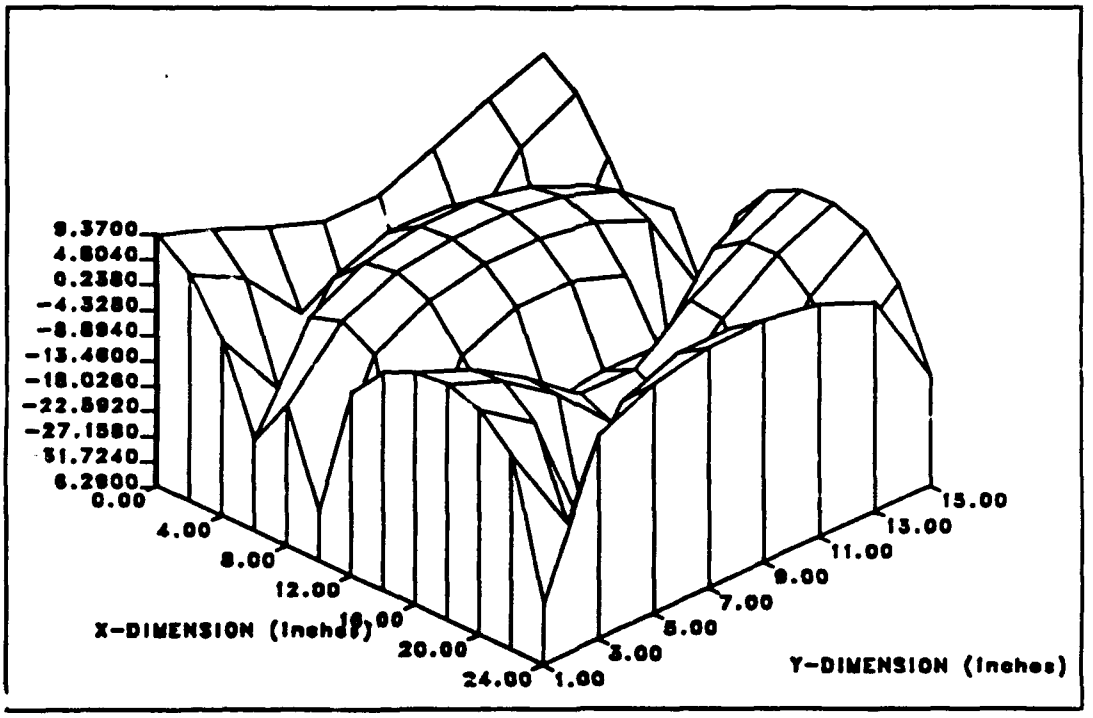

Figure 5.27: Three-dimensional plot of 1,3 and 4,1 modes excited by a 60.5 Hz signal

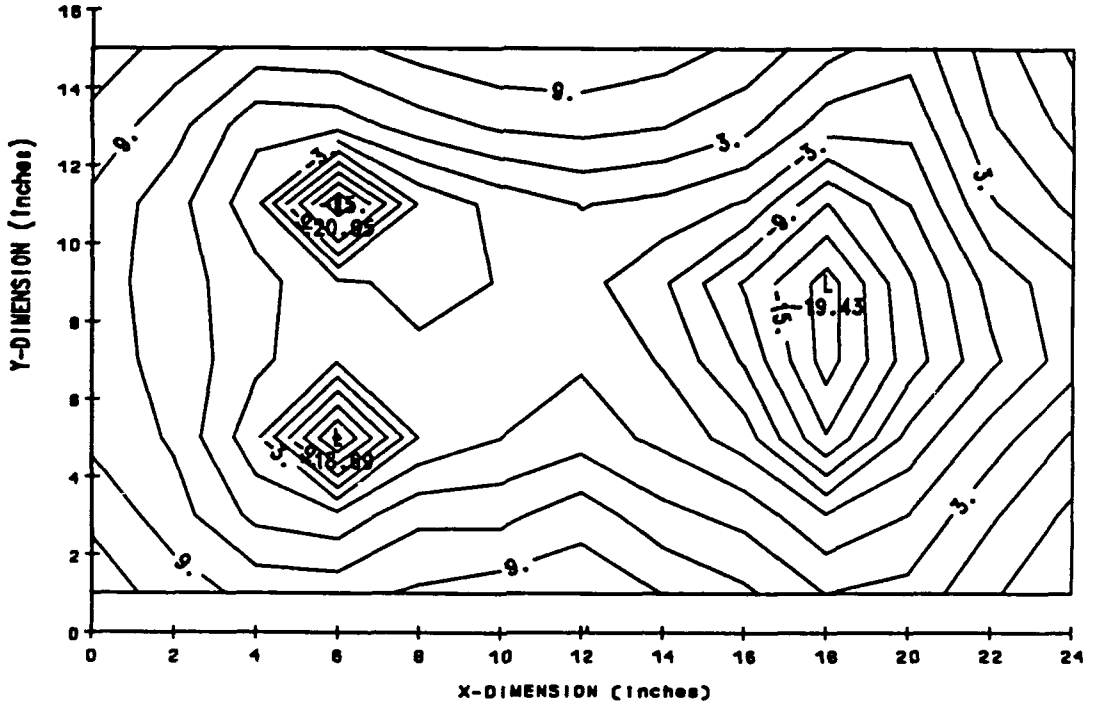

Figure 5.28: Contour plot of 3,2 mode with no shakers

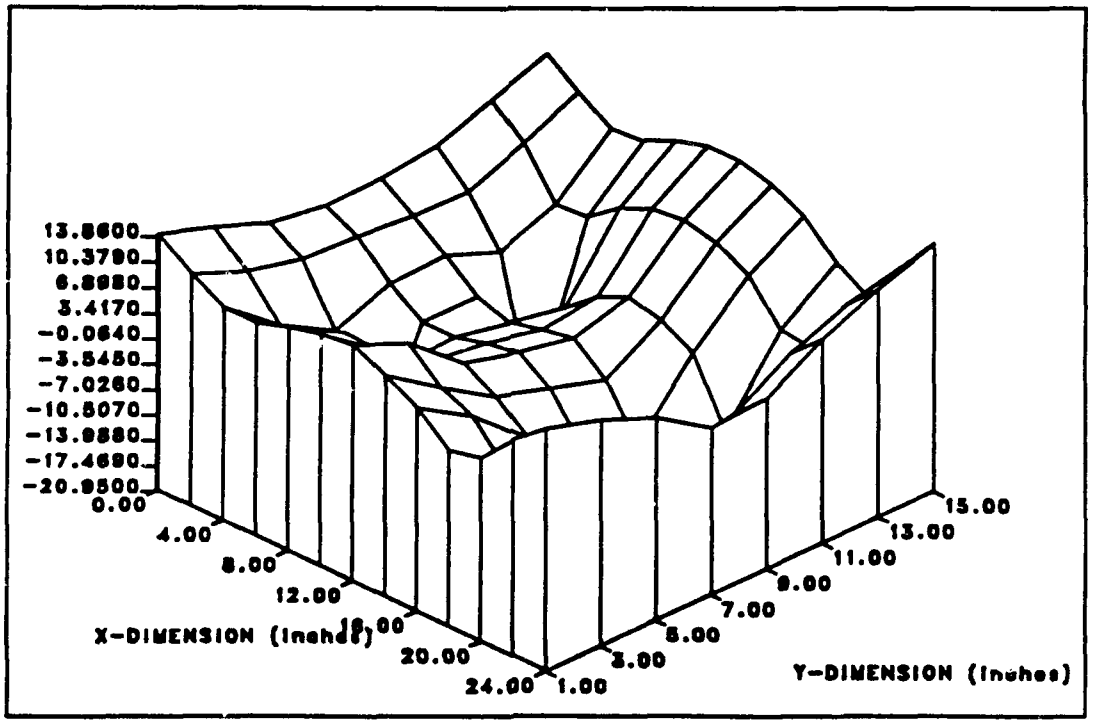

Figure 5.29: Three-dimensional plot of 3,2 mode with no shakers

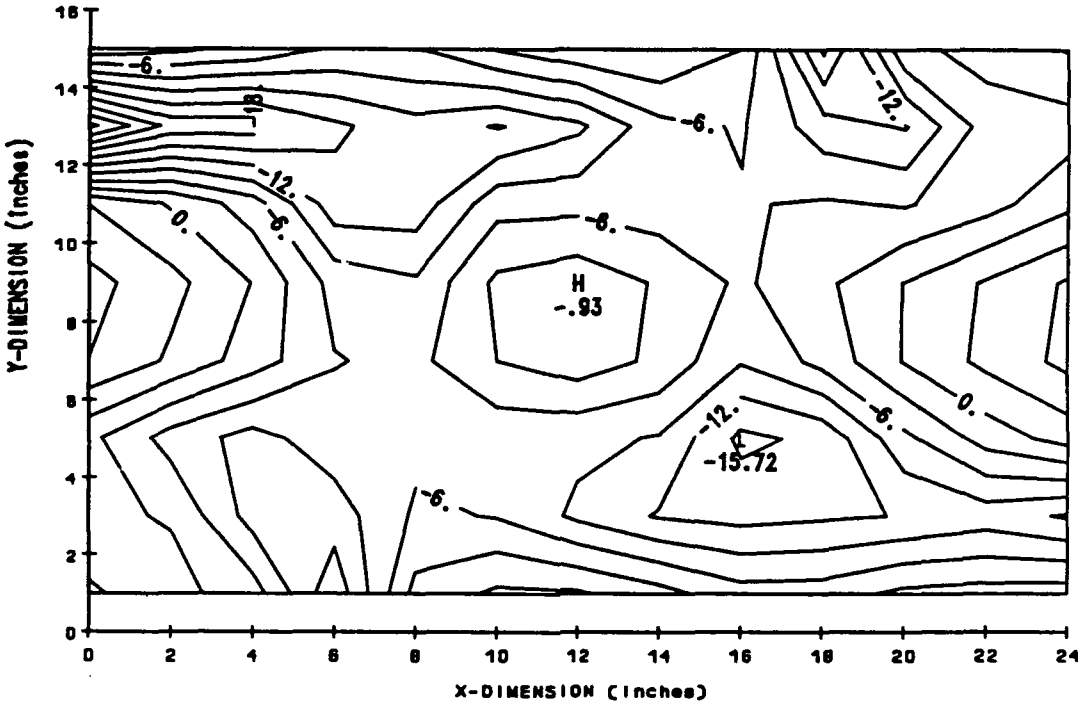

Figure 5.30: Contour plot of 3,2 mode with shakers attached

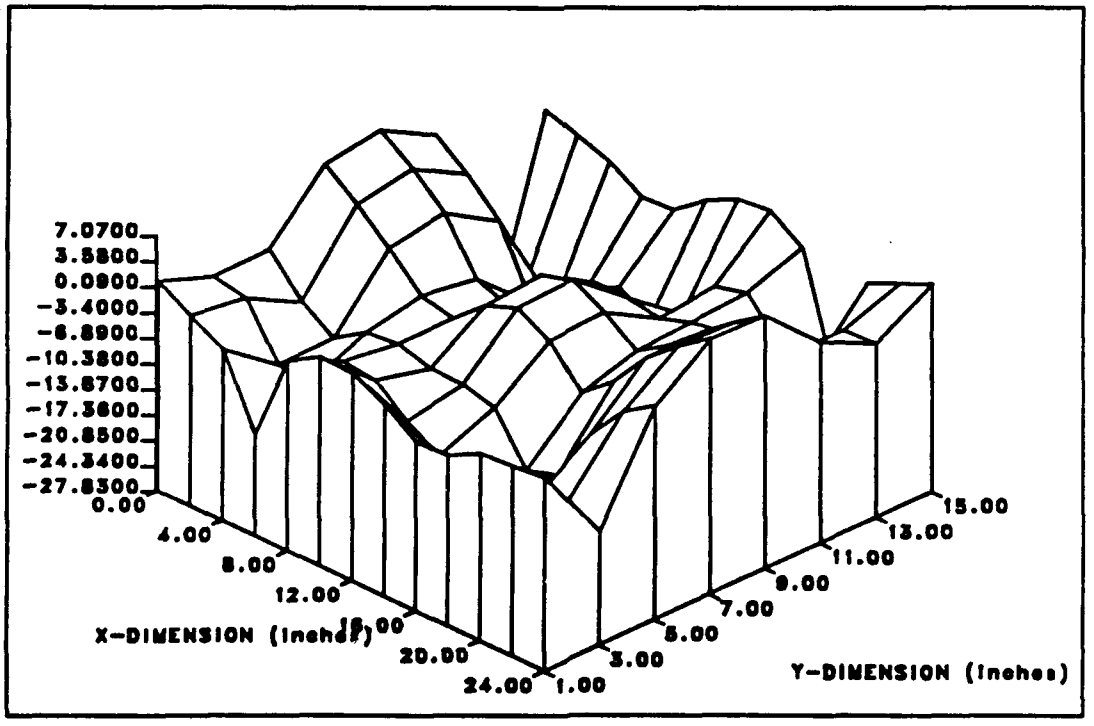

Figure 5.31: Three-dimensional plot of 3,2 mode with shakers attached

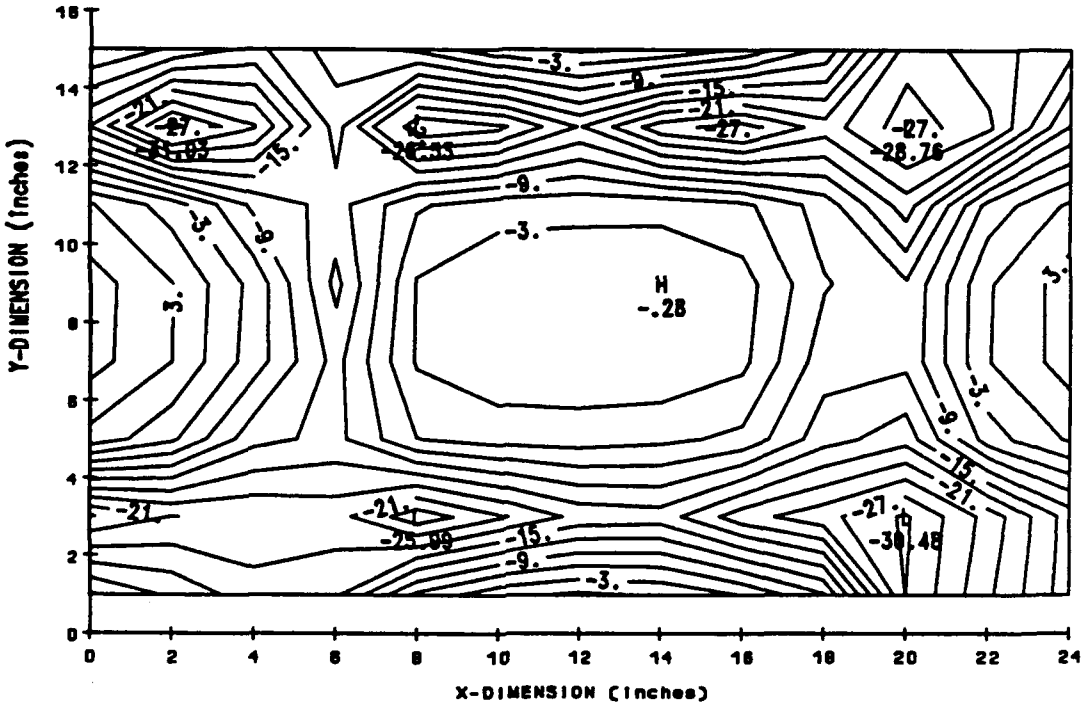

Figure 5.32: Contour plot of four-channel control of 3,2 mode

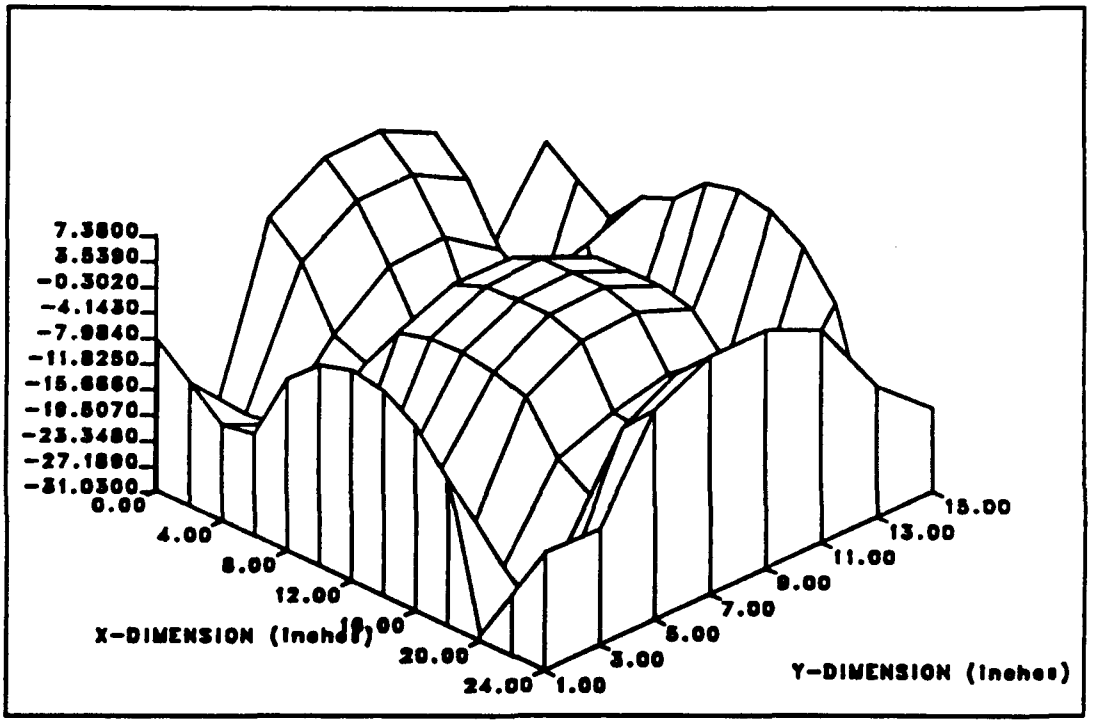

Figure 5.33: Three-dimensional plot of four-channel control of 3,2 mode

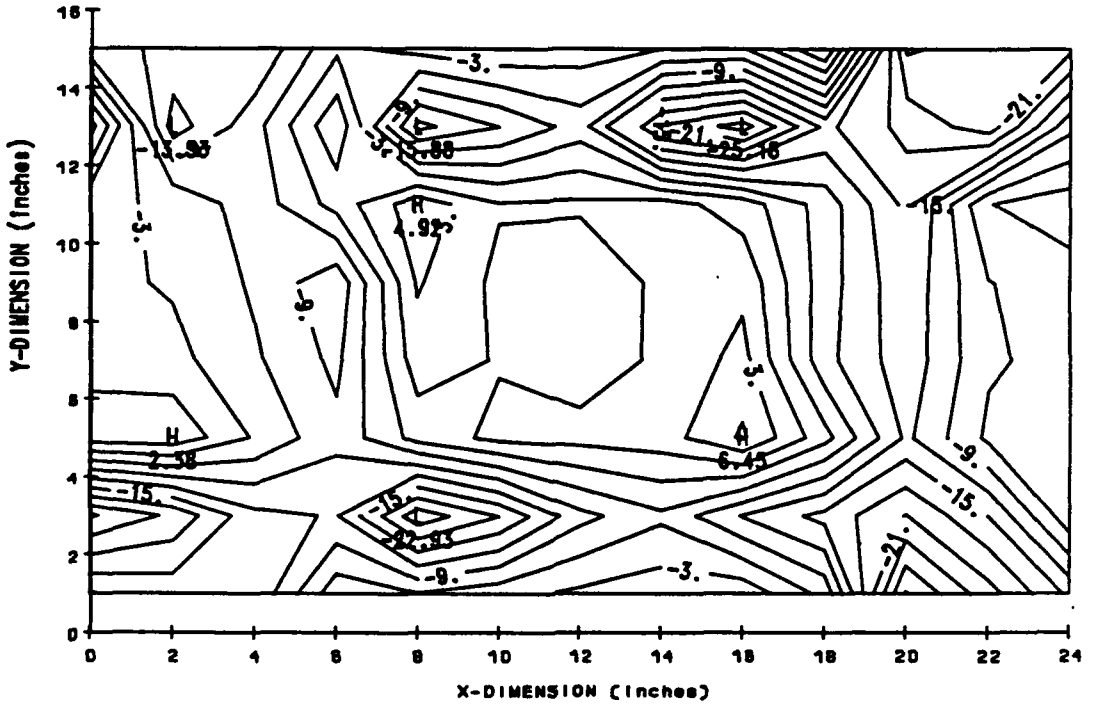

Figure 5.34: Contour plot of four-channel reduction of 3,2 mode

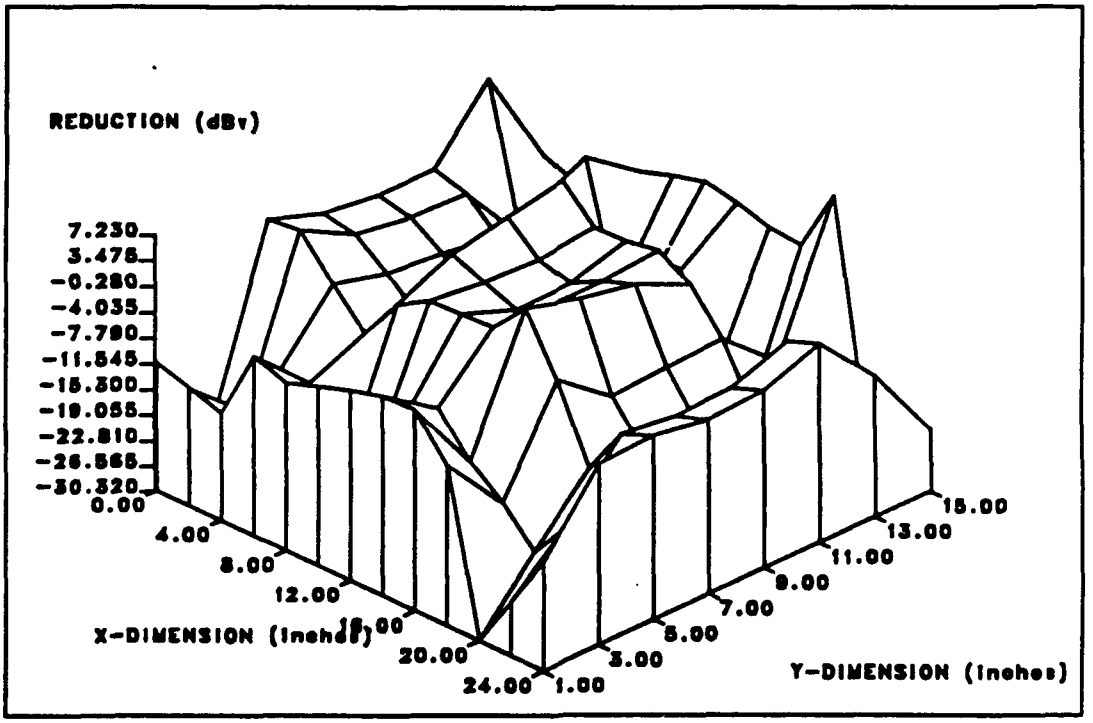

Figure 5.35: Three-dimensional plot of four-channel reduction of 3,2 mode

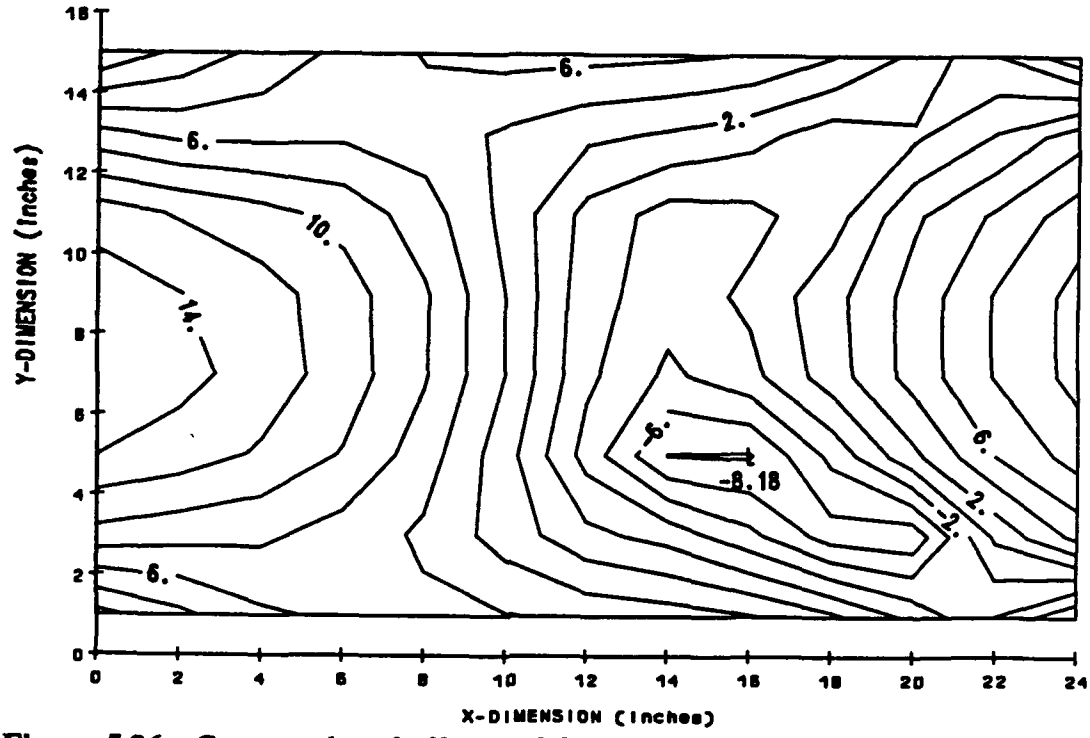

Figure 5.36: Contour plot of effective 2,2 mode

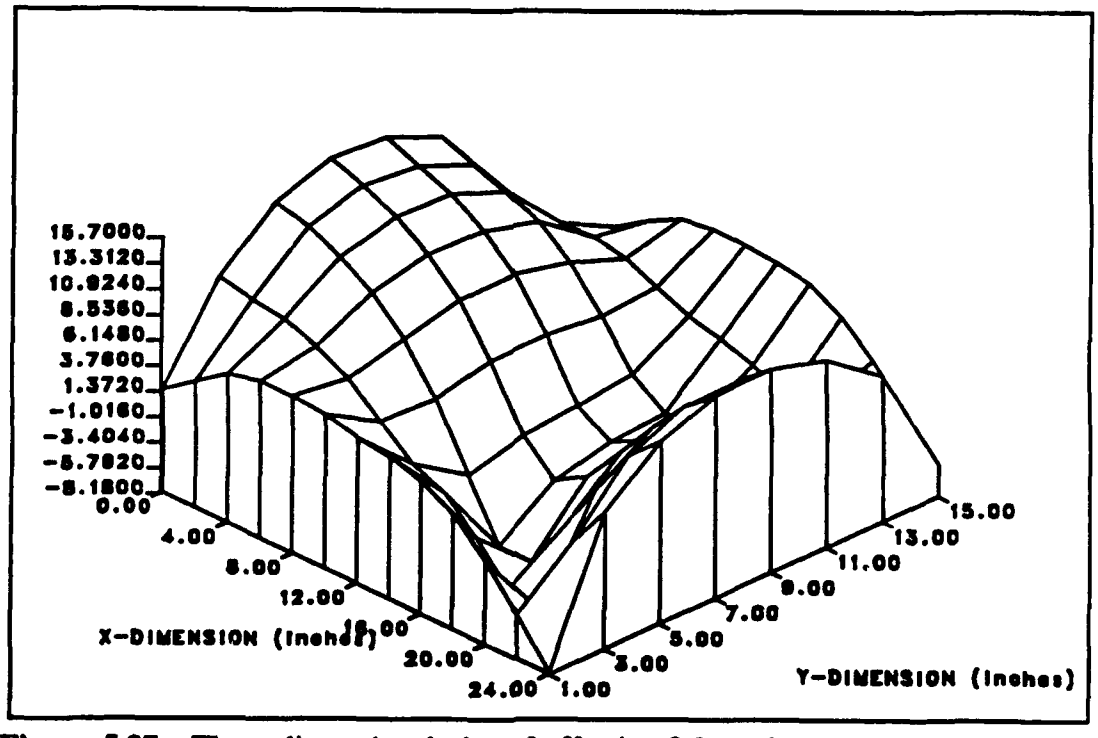

Figure 5.37: Three-dimensional plot of effective 2,2 mode

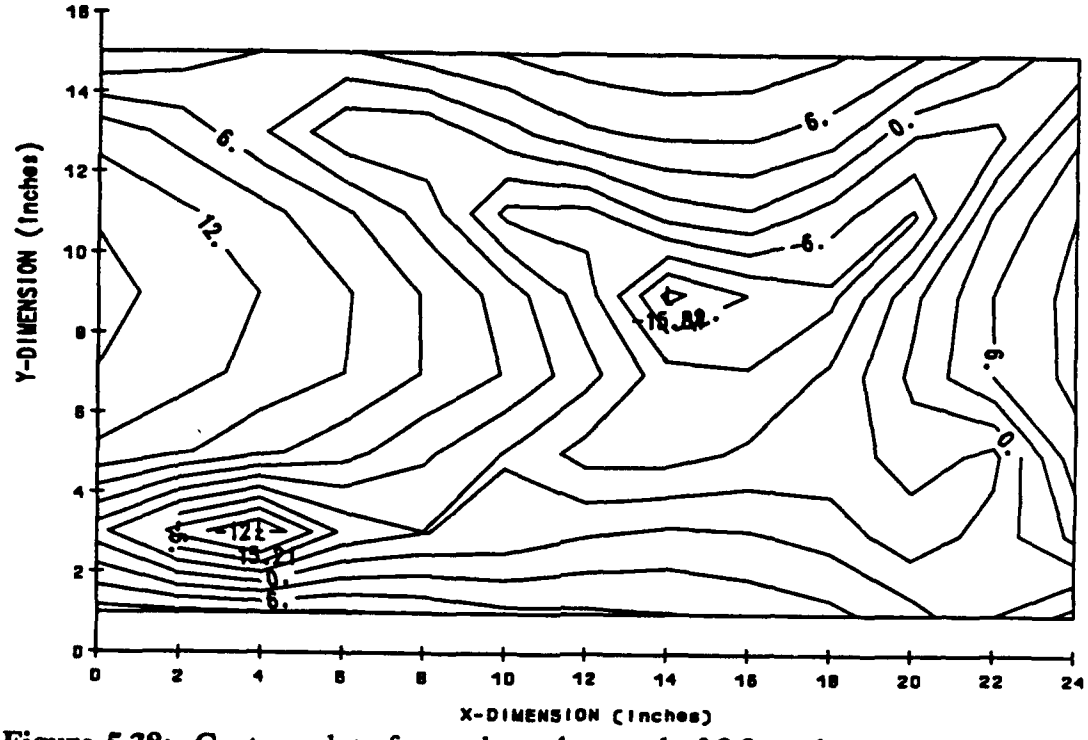

Figure 5.38: Contour plot of two-channel control of 2,2 mode

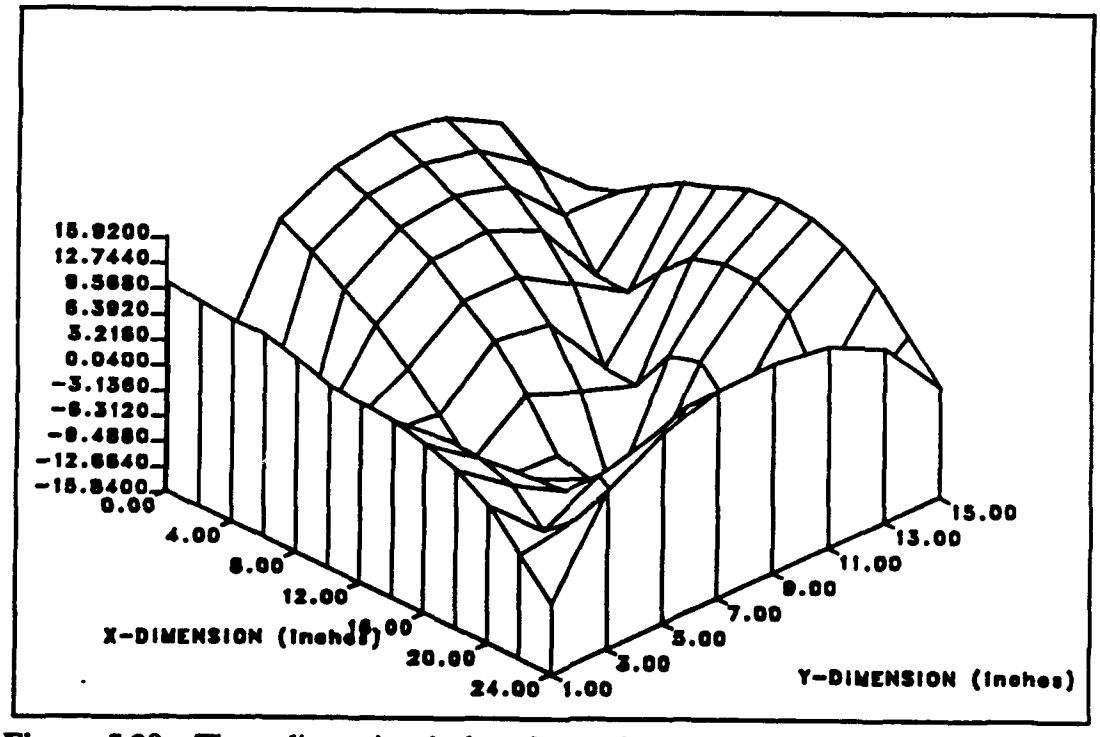

Figure 5.39: Three-dimensional plot of two-channel control of 2,2 mode

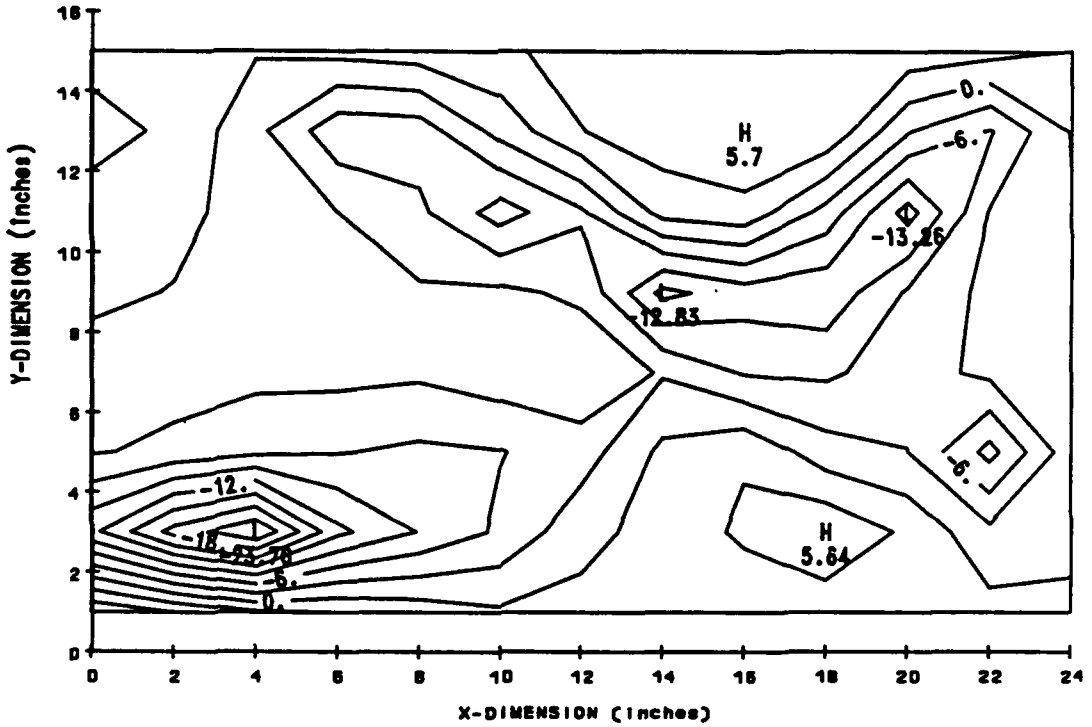

Figure 5.40: Contour plot of two-channel reduction of 2,2 mode

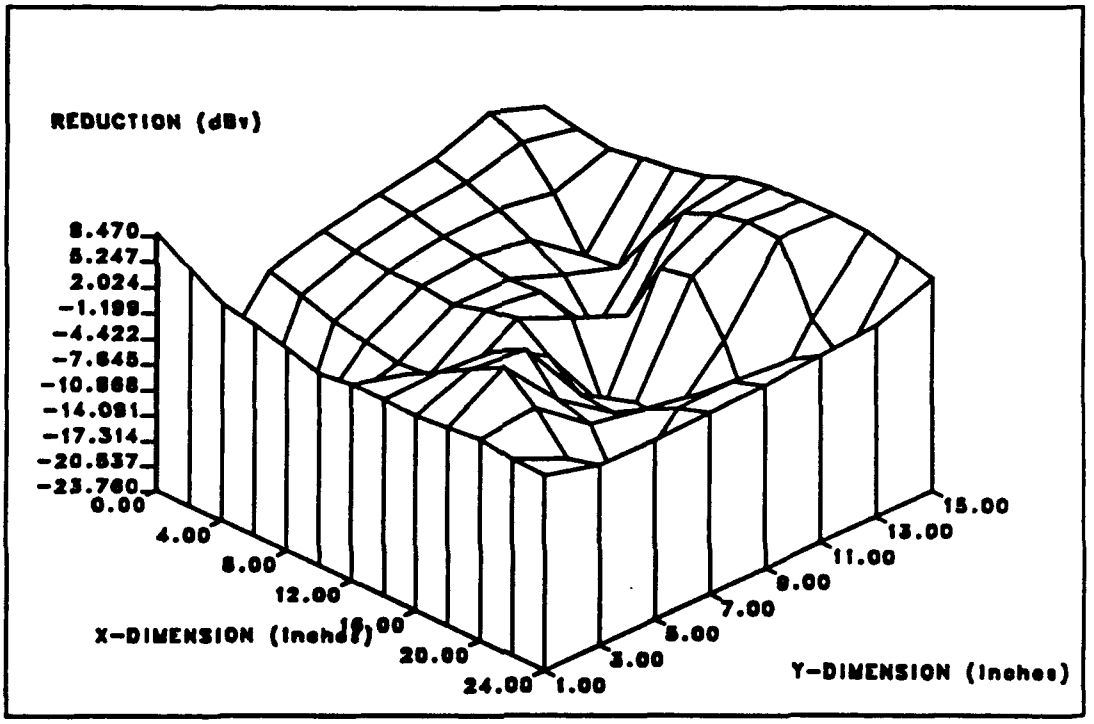

Figure 5.41: Three-dimensional plot of two-channel reduction of 2,2 mode

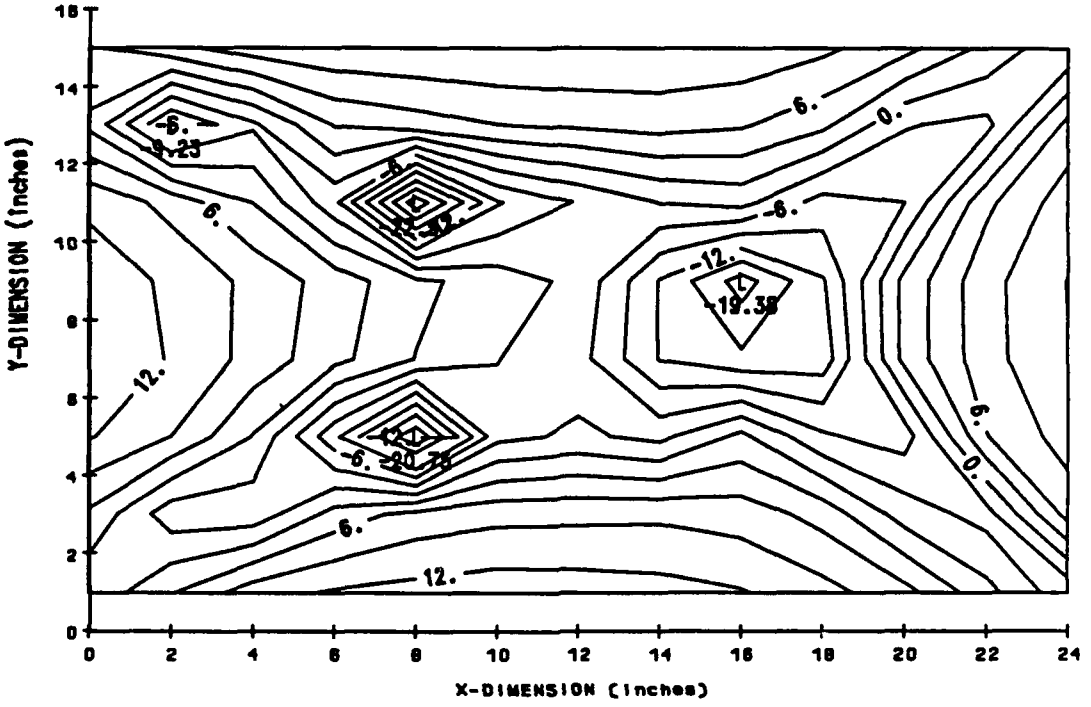

Figure 5.42: Contour plot of four-channel control of 2,2, mode

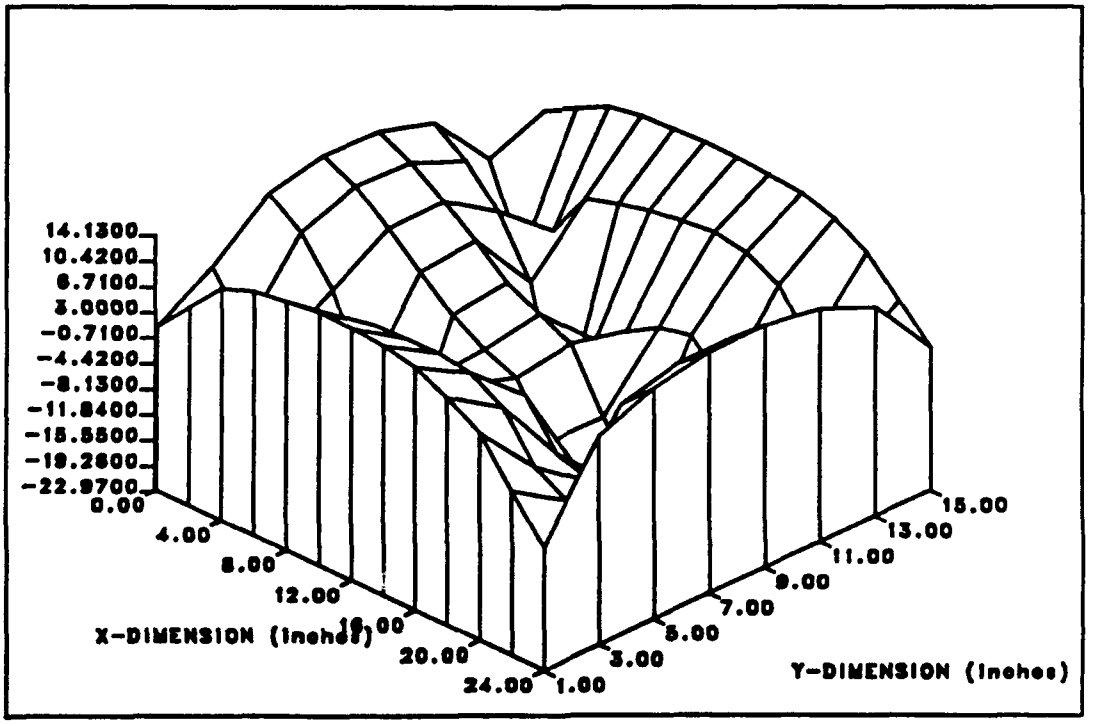

Figure 5.43: Three-dimensional plot of four-channel control of 2,2 mode

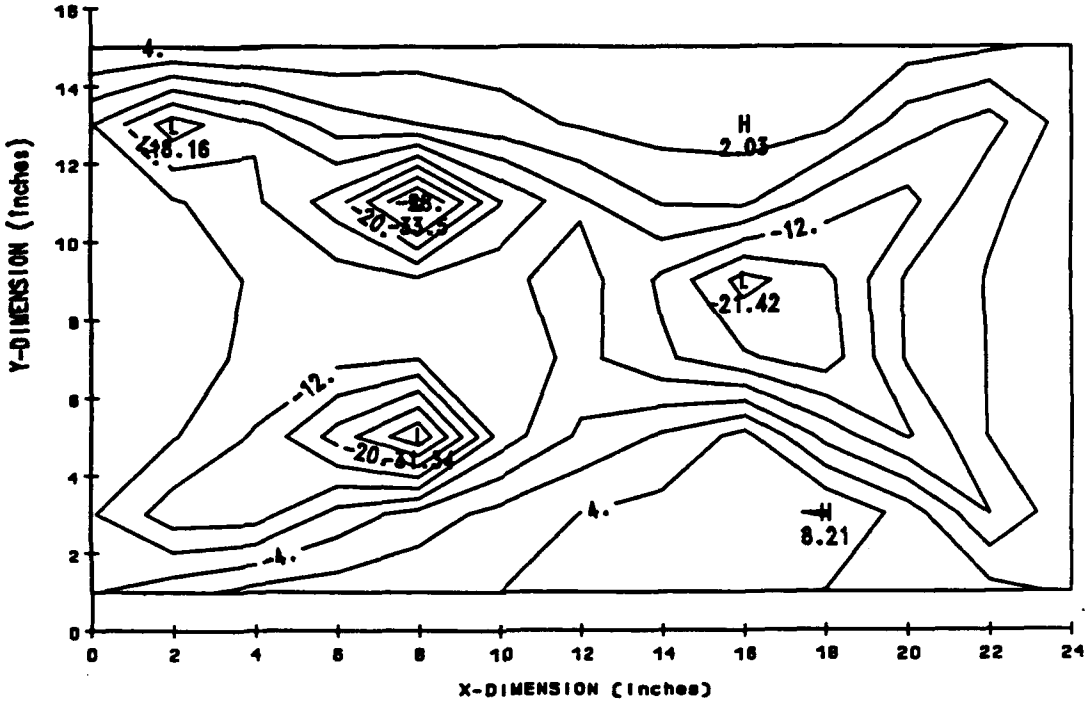

Figure 5.44: Contour plot of four-channel reduction of 2,2 mode

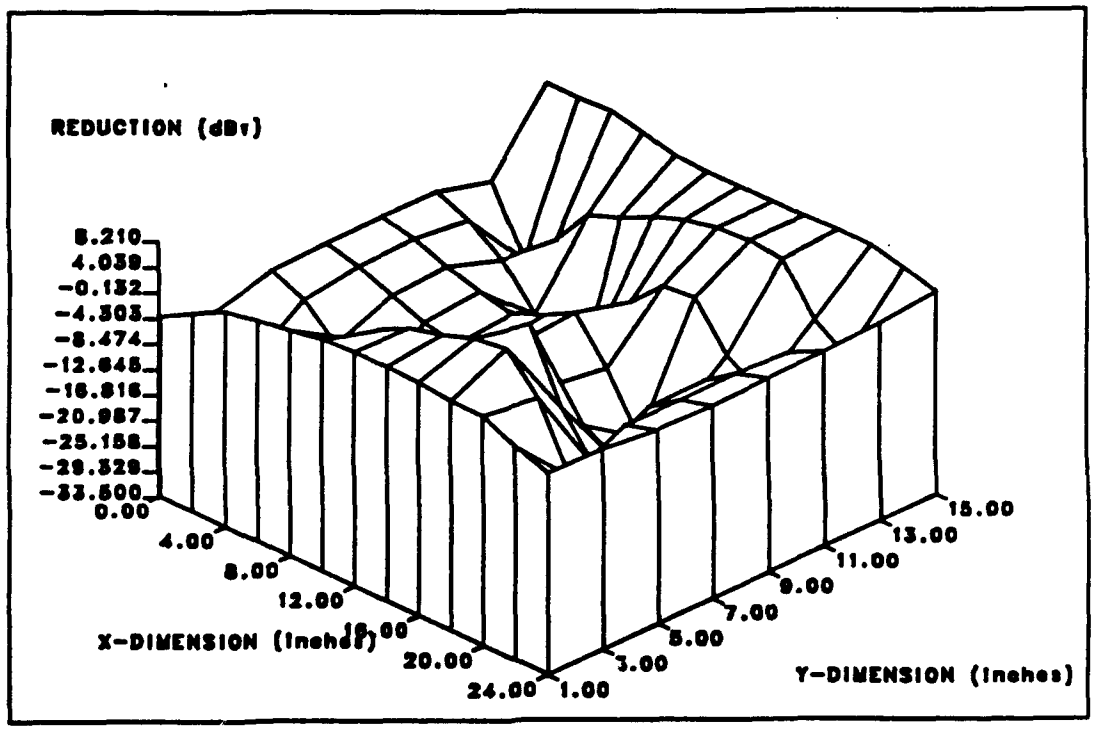

Figure 5.45: Three-dimensional plot of four-channel reduction of 2,2 mode

Chapter 6

CONCLUSIONS AND RECOMMENDATIONS

The objective of this thesis was to study the effects of real-time multichannel adaptive control when applied to reducing structural vibration of a distributed system. The system chosen was a metal plate mounted to a rigid foundation with springs, with adaptive control performed by a LMS-based control algorithm. Problems associated with such multiple processes were discussed, and solutions to such problems were presented. The problem of feedback instability was discussed and a solution arrived at through *a priori* feedback compensation filters. The intent of this thesis was to provide an advanced method of vibration control to apply to multiple transmission paths on a vibrating structure.

In addition to canceling vibrations transmitted to a rigid foundation, global vibration reduction was examined. Modal patterns of the plate system were observed, and provided additional insight into areas such as: ideal actuator/sensor location, modal shifting, and effects of inactive control shakers on boundary conditions.

When the system was assembled, the objective of the study was to reduce vibrations at the transmission paths. Therefore, error sensors were located at the transmission points and control actuators were located as near to the corners as possible.

This provided excellent localized reduction when the modal patterns produced antinodes at the error sensors. However, it was found that when error sensors were located near nodal lines, a more uniform or global, but less effective, reduction was the result. This indicates that when error sensors are located near antinodes, changes in modal patterns result. However, when the error sensors intercept nodal lines, reduction, with little effect on the vibrating modal pattern of the plate, will result.

The controller was shown to have a frequency range for which it was effective. The highest frequency of this effective range corresponds to half of the sampling frequency of the controller as given by the Nyquist criterion [41]. In the case of this thesis, this upper frequency corresponded to 500 Hz due to hardware limitations. For vibration control above this frequency, passive techniques exist and provide adequate attenuation of such high frequency vibrations. Proper combinations of adaptive and passive techniques should therefore provide adequate attenuation throughout an entire frequency range of interest. Such a system should therefore be effective in reducing transmitted vibrations from a source, which contacts a foundation at multiple locations.

The adaptive control algorithm used in this study was complex, as described in chapter 3. Observation of this algorithm provided an interesting area of study to be further researched. The adaptive μ algorithm was not used initially in this study, but did provide better stability to the system. Also, equation (3.31) provides a means for calculating a convergence parameter for the projection algorithm, based upon a ratio of convergence of the projection algorithm to the convergence of the LMS filter. It was found that this equation did not properly estimate a stable value for the projection

algorithm's convergence parameter, and that a more conservative value had to be chosen. This may be due to the fact that it was assumed, in equation (3.29), that the power of the output signal of the LMS filter had the same power as that of the input signal to the LMS filter. This may be true at the algorithm's execution time, if leading tap coefficients are set to a large constant value, but may not hold as the algorithm is allowed to converge. An extensive study into the area of simultaneous multiple adaptive processes may provide a better means of predicting convergence parameters for such control situations.

The major limitation encountered in this thesis was hardware. A faster digital signal processing board would have provided better results, as it would have allowed over-sampling. In the development of the control software, over-sampling was shown to provide faster convergence times, as it allowed the computer more calculations per unit time when compared to simple Nyquist criterion sampling frequencies. As the number of channels was increased to four, and the order of the filters was maintained, such over-sampling frequencies could not be used as the algorithm calculation time exceeded the sampling period. The speed of the signal processing board also became a limiting factor in the case of feedback compensation. Due to the physical layout of the control system, described in chapter 4, the data bus approached 3 feet in length. When the feedback compensation filters, located at the end of this bus, were accessed by the processing chip, data was occasionally misread, due to the high speed at which this bus was operating. Additional hardware limitations included the control actuators and accelerometers. Due to the limited dynamic range of both the shakers and accelerometers, excitation amplitudes had to be kept at a relatively small value. If the linear range of these devices

is exceeded, the control algorithm approaches instability and thus causes the system to diverge.

Hardware also imposed limitations on the effectiveness of the controller. Due to the dispersive medium of the plate, phase speed through the structure increases as the frequency increases. Therefore, there is a cutoff frequency at which the time required to calculate and actuate the control shakers surpasses the propagation time through the plate system. This occurred at a relatively low frequency, indicating that the controller was not suitable for the control of wideband random excitation signals. Algorithms with reduced convergence times could prove effective in increasing the performance of the controller. A study by Hodgkiss [42] showed that algorithms such as the Lattice Adaptive Filter converge more rapidly than that of the LMS, but are more computationally complex.

Additional recommendations for continued research in the area of adaptive vibration control include a method of unobtrusively measuring vibrations for error signals to the algorithm, two-dimensional Fourier transforms of wave numbers, and ideal locations for error sensors and control actuators.

An unobtrusive error sensor, such as a laser interferometer, would allow the error sensor to be moved without changing the boundary conditions of the system. Such a system would allow one to observe the performance of the controller as a function of changes in error sensor location, and changes in the surface area of the error sensor. Additional features include an easy way to determine modal analysis for the vibrating structure.

A two-dimensional spatial Fourier transform of the modal analysis data would

allow one to determine the contribution of various modes. This would be extremely effective in the case of the thin plate used in this thesis, because it was difficult to determine which modes the plate was vibrating in when control actuators were attached to the system. From such a study, the optimal location of shakers and error sensors could be more easily determined, to achieve both global and localized reduction effectively.

Although the applications of adaptive control are still relatively new, important progress has been made. This study demonstrates promising results, as well as current limitations of technology, when applied to a problem such as vibration control. The problem addressed in this study constitutes a realistic situation in which a distributed system contacts a foundation at multiple locations. Adaptive vibration control provides effective reduction of transmitted vibrations in this experiment, and holds promising results for low-frequency structural vibration control.

References

[1] P. Lueg, "Verfahren zur Dampfung von Schallschwingungen," German Patent, DRP No. 655,508, filed: Jan. 27,1933; issued: Dec. 30, 1937.

[2] P. Lueg, "Process of Silencing Sound Oscillations," United States Patent, No. 2,043,416, filed: Mar. 8, 1934; issued: June 9, 1936.

[3] H.F. Olson and E.G. May, "Electronic Sound Absorber," Jour. Acoustical Soc. of America, Vol. 25, No. 6 (1953), pp. 1130-1136.

[4] H.F. Olson, "Electronic Control of Noise, Vibration, and Reverberation, " Jour. Acoustical Soc. of America, Vol. 28, No. 5 (1956), pp. 966-972.

[5] M.J.M. Jessel and G.A. Mangiante, "Active Sound Absorbers in an Air Duct," Journal of Sound and Vibration, Vol. 23, No. 3 (1972), pp. 383-390.

[6] M.A. Swinbanks, "The Active Control of Sound Propagation in Long Ducts," Journal of Sound and Vibration, Vol. 27, No. 3 (1973), pp.411-436.

[7] J.H.B. Poole and H.G. Leventhall, "An Experimental Study of Swinbanks' Method of Active Attenuation of Sound Ducts," Journal of Sound and Vibration, Vol. 49, No. 2 (1976), pp. 257-266.

[8] J.H.B. Poole and H.G. Leventhall, "Active Attenuation of Noise in Ducts, " Journal of Sound and Vibration, Vol. 57, No. 2 (1978), pp. 308-309.

[9] G.G.B Chaplin and R.A. Smith, "The Sound of Silence-The Silencing of Diesel Exhausts by Out-of-Phase Cancellation Using a Microprocessor Has Now Been Achieved," Engineering (London), No. 218 (1978), pp. 672-673.

[10] G.C. Goodwin and K.S. Sin, Adaptive Filtering Prediction and Control (Englewood Cliffs, NJ: Prentice-Hall, 1984), p. xi.

[11] B. Widrow, J.R. Glover, Jr., J.M. McCool, J. Kaunitz, C.S. Williams, R.J. Hearn, J.R. Zeidler, E. Dong, Jr., and R.C. Goodlin, "Adaptive Noise Canceling: Principles and Applications," Proceedings of the IEEE, Vol. 63, No. 12 (1975), pp. 1692-1716.

[12] B. Widrow and S.D. Stearns, Adaptive Signal Processing (Englewood Cliffs, NJ: Prentice-Hall, 1985), pp. 5-6.

[13] G.E. Warnaka and J. Tichy, "Acoustic Mixing in Active Attenuators," Proceedings of Inter-Noise 80, Miami, Florida (December 1980), pp. 683-688.

[14] G.E. Warnaka, J. Tichy, and L.A. Poole, "Improvements in Adaptive Active Attenuators," Proceedings of Inter-Noise 81, Amsterdam, the Netherlands (October 1981), pp. 307-310.

[15] G.E. Warnaka, L.A. Poole and J. Tichy, "Transient Response in Active Systems," Proceedings of Inter-Noise 82, San Francisco, CA (May 1982), pp.427-430.

[16] G.E. Warnaka, J.M. Zalas, J. Tichy, and L.A. Poole, "Active Control of Noise in Interior Spaces," Proceedings of Inter-Noise 83, Edinburgh, U.K. (July 1983), pp. 415-418.

[17] P.A. Nelson and S.J. Elliot, "Active Minimisation of Acoustic Fields," (Institute of Sound and Vibration Research, ISVR Technical Report 146, May 1987) pp. 1-39.

[18] P.A. Nelson, A.R.D. Curtis, S.J. Elliott and A.J. Bullmore, "The Minimum Power Output of Free-Field Point Sources and the Active Control of Sound," Journal of Sound and Vibration, Vol. 116, No. 3 (1987), pp. 397-414.

[19] J.S. Burdess and A.V. Metcalfe, "The Active Control of Forced Vibration Produced by Arbitrary Disturbances," Journal of Vibration, Acoustics, Stress and Reliability in Design, Vol. 107 (1985), pp. 33-37.

[20] S. Lee and A. Sinha, "Design of an Active Vibration Absorber," Journal of Sound and Vibration, Vol. 109, No. 2 (1986), pp. 347-352.

[21] T. Takagami and Y. Jimbo, "Study of an Active Vibration Isolation System-A Learning Control Method," Proceedings of Inter-Noise 84, Honolulu, HA (December 1984), pp. 503-508.

[22] T. Takagami and Y. Jimbo, "Study of an Active Vibration Isolation System-A Learning Control Method," Journal of Low Frequency Noise and Vibration, Vol. 4, No. 3 (1985), pp.104-119.

[23] R.G. Owen and D.I. Jones, "Multivariable Control of an Active Anti-Vibration Platform," IEEE Transactions on Magnetics, Vol. MAG-22, No. 5 (1986), pp. 523-525.

[24] E. Anton and H. Ulbrich, "Active Control of Vibrations in the Case of Asymmetrical High-Speed Rotors by Using Magnetic Bearings," Journal of Vibration, Acoustics, Stress, and Reliability in Design, Vol. 107 (1985), pp. 410-415.

[25] C.R. Burrows and M.N. Sahinkaya, "Vibration Control of Multi-Mode Rotor-Bearing Systems," Proceedings of the Royal Society of London, Vol. A 386 (1983), pp.77-94.

[26] T. Bailey and J.E. Hubbard Jr., "Distributed Piezoelectric-Polymer Active Vibration Control of a Cantilever Beam," Journal of Guidance and Control, Vol. 8, No. 5 (1985), pp. 605-611.

[27] B.E. Schäfer and H. Holzach, "Experimental Research on Flexible Beam Modal Control," Journal of Guidance and Control, Vol. 8, No. 5 (1985), pp.597-604.

[28] N. Tanaka and Y. Kikushima, "On the Suppression of Ground Vibration by Active Force Controller (Suppression of Exciting Force by Feedforward Control)," Bulletin of the JSME, Vol. 26, No. 215 (1983), pp. 839-847.

[29] N. Tanaka and Y. Kikushima, "On the Suppression of Ground Vibration by Active Force Controller (3rd report; Suppression of Exciting Force by Rigid Support Method)," Bulletin of the JSME, Vol. 28, No. 244 (1985), pp. 2378-2385.

[30] N. Tanaka and Y. Kikushima, "On the Suppression of Ground Vibration by Active Force Controller (4th report; On the Hybrid Force Control)," Bulletin of the JSME, Vol. 29, No. 251 (1986), pp. 1548-1556.

[31] N. Tanaka and Y. Kikushima, "On the Suppression of Ground Vibration by Active Force Controller (5th report; Experiment of the Hybrid Force Control Method)," Bulletin of the JSME, Vol. 29, No. 251 (1986), pp. 1557-1563.

[32] S.D. Sommerfeldt, "Adaptive Vibration Control of Vibration Isolation Mounts Using an LMS-Based Control Algorithm," (Ph.D. Thesis, The Pennsylvania State University, University Park, PA, 1989).

[33] A.W. Leissa, "The Free Vibration of Rectangular Plates," Journal of Sound and Vibration, Vol. 31, No. 3 (1973), pp. 257-293.

[34] L. Meirovitch, Analytical Methods in Vibrations (The Macmillan Company, Collier-Macmillan Limited, London, 1967), pp. 179-189.

[35] L.E. Kinsler, A.R. Frey, A.B. Coppens, and J.V. Sanders, Fundamentals of Acoustics (New York, NY: John Wiley and Sons, Inc., 1982), p. 461.

[36] S.T. Alexander, Adaptive Signal Processing Theory and Applications (New York, NY: Springer-Verlag New York Inc., 1986), pp. 74-83.

[37] B. Widrow and S.D. Stearns, Adaptive Signal Processing (Englewood Cliffs, NJ: Prentice-Hall, 1985), p. 22.

[38] B. Widrow and S.D. Stearns, Adaptive Signal Processing (Englewood Cliffs, NJ: Prentice-Hall, 1985), pp. 288-294.

[39] G.C. Goodwin and K.S. Sin, Adaptive Filtering Prediction and Control (Englewood Cliffs, NJ: Prentice-Hall, 1984), pp. 49-58.

[40] D.J. DeFatta, J.G. Lucas, and W.S. Hodgkiss, Digital Signal Processing: A System Design Approach, (New York, NY: John Wiley and Sons, Inc., 1988), pp. 601-604.

[41] A.V. Oppenheim and R.W. Schafer, Digital Signal Processing (Englewood Cliffs, NJ: Prentice-Hall, 1975), pp.26-30.

[42] W. Hodgkiss, Jr. and J.A. Presley, Jr., "Adaptive Tracking of Multiple Sinusoids Whose Power Levels are Widely Seperated," IEEE Transactions on Acoustics, Speech, and Signal Processing, Vol. ASSP-29, No. 3, June 1981, pp. 710-721.